01 Feb 1998

Design of automotive structural components using high strength sheet steels transformed section method for the calculation of yield moment of cold-formed steel hybrid beams

Chi-Ling Pan

Wei-wen Yu
Missouri University of Science and Technology, wwy4@mst.edu

Civil Engineering Study 98-1
Cold-Formed Steel Series

Twenty-Second Progress Report

DESIGN OF AUTOMOTIVE STRUCTURAL COMPONENTS
USING HIGH STRENGTH SHEET STEELS

TRANSFORMED SECTION METHOD FOR THE CALCULATION OF YIELD MOMENT OF COLD-FORMED STEEL HYBRID BEAMS

by

Chi-Ling Pan
Consultant
Chaoyang University of Technology

Wei-Wen Yu
Project Director
University of Missouri-Rolla

A Research Project Sponsored by the American Iron and Steel Institute

February 1998

Department of Civil Engineering
University of Missouri-Rolla
Rolla, Missouri

TABLE OF CONTENTS

LIST OF TABLES

LIST OF TABLES (cont.)

LIST OF FIGURES

I. Introduction

It has been recognized that material properties and stress-strain relationships of sheet steel can be influenced by the strain rate. Because the member strength is also influenced by dynamic loading, a large number of research projects were conducted for a variety of structural members under specified loading conditions during past three decades.

In cold-formed steel design, local buckling is one of the major design features because of the use of large width-to-thickness ratios for compression elements. For the purpose of determining the load-carrying capacity of automotive components, the effective width approach has been used. In view of the fact that the design criteria for effective design widths included in the current AISI Automotive Steel Design Manual [1] are primarily based on the results of static tests of cold-formed steel members corresponding to a strain rate approximately 1.7×10^{-6} in./in./sec., an investigation was conducted at University of Missouri-Rolla (UMR) since 1989 under the sponsorship of the American Iron and Steel (AISI) to study the validity of these effective design width formulas for the design of cold-formed steel automotive components subjected to dynamic loads (Pan and Yu [2], Kassar and Yu [3]).

The results presented in Reference [2] showed that the effective cross-sectional area calculated on the basis of the dynamic yield stresses can be employed in the determination

of ultimate loads. Because previous research projects were limited only to the structural members which were fabricated from one material or assembled with the same material in a given section, and it is known that the application of higher strength steels to structures often results in significant material-cost savings, the study of beam specimens fabricated from two types of sheet steels subjected to dynamic loads was initiated in October 1993. In this study, a total of 72 beam specimens fabricated from two different sheet steels (25AK and 50 SK) were tested under different strain rates to study the structural strength and behavior of hybrid sections. The strain rates used in the beam tests were from 10^{-4} to 10^{-2} in./in./sec.. The test results of hybrid beam specimens were presented in the Twentieth Progress Report [4].

In 1964, Ronald Frost and Charles Schilling [5] studied the behavior of hybrid plate girders consisting of higher-strength steel flanges connected with lower-strength steel webs, under pure bending and combined shear and bending. They suggested that the maximum bending strength of a hybrid beam may be considered to be (1) the moment causing the cross section to become fully plastic or (2) the moment causing initial yielding in the flange, because it has been demonstrated that the yielding which occurs in the webs of hybrid beams has little effect on the behavior of such beams.

Pan and Yu [4] concluded that the available effective design width formulas using dynamic material properties can be adequately used for the design of hybrid structural

members fabricated from two different materials subjected to dynamic loads. In addition, the procedures discussed in the 20th Progress Report [4] can provide a reasonable approach for calculating the critical local buckling moment, the yield moment, and the ultimate moment. However, due to the complexity for the calculation of ultimate moment using inelastic reserve capacity and the possible excessive deflection, it is suggested that for practical design, the yield moment can be used for the load-carrying capacity of hybrid beams. In this report, an alternative computing procedure was developed and utilized in the calculation of load-carrying capacity of cold-formed steel hybrid beams.

The tests of hybrid beam specimens subjected to dynamic loading conditions are discussed in Chapter 2 of this report. In Chapter 3, the alternative procedures for calculating the flexural strength of hybrid beams are presented. Finally, the research findings are summarized in Chapter 4.

II. Experimental Investigation

A. GENERAL

This research project was sponsored by the American Iron and Steel Institute (AISI) at University of Missouri-Rolla (UMR). The latter phase of the project dealt with strength and behavior of cold-formed steel hybrid beams under dynamic loads. In the first phase of the project, the material properties of two selected sheet steels (25AK and 50SK) were tested and studied. The test results of the static and dynamic mechanical properties in tension and compression under different strain rates were established. Seventy-two beam specimens assembled with these two selected sheet steels were studied experimentally and analytically under dynamic loads in the second phase of the project. The objective of this phase of the study is mainly to develop an alternative approach for calculating the yield moment of cold-formed steel hybrid beams under dynamic loading conditions.

B. MATERIAL PROPERTIES

The materials used in this investigation were 25AK and 50SK sheet steels with nominal yield strengths equal to approximately 25 and 50 ksi, respectively. These two materials have been tested for establishing the mechanical properties in tension and compression in the longitudinal and transverse directions under different strain rates of 10^{-4}, 10^{-2}, 10^{-1}, and 1.0 in./in./sec.. The mechanical properties of these two types of sheet steels were presented in the Seventeenth Progress Report [6]. Tables 2.1 and 2.2

summarize the average values of mechanical properties including yield strength (F_y) in tension and compression, proportional limit (F_{pr}), tensile strength (F_u), and elongation in 2-inch gage length for 25AK and 50SK sheet steels which were tested under four different strain rates. The lower yield point of the stress-strain diagram was used to determine the yield strength for 50SK sheet steel. For 25AK sheet steel, the yield strength was determined by the 0.2 % offset method because of the gradual yielding type of stress-strain relationship. The nominal thicknesses of the 25AK and 50SK sheet steels were 0.078 inch and 0.074 inch, respectively. Based on the material test results, empirical equations for characteristic mechanical properties were derived and presented in the Eighteenth Progress Report [7] and References 4 and 8. The dynamic tensile and compressive proportional limits and yield strengths obtained from the material tests were used to evaluate the bending strength of beam specimens.

C. BEAM SPECIMENS

The configuration of hybrid beam specimens is shown in Figure 2.1. The designation of test specimens is presented in Table 2.3. As shown in Figure 2.1, a hat section and a plate were assembled by attaching the plate to the unstiffened flanges of the hat section to form a hat-shaped beam. All test specimens were fabricated by using spot welded connections. Spot welds of 1-inch spacing were used on each unstiffened flange of hat sections for all specimens regardless the length of specimens. In order to study the behavior and strength of stiffened compression elements, the webs of hat-shaped beam

specimens were designed to be fully effective without web buckling and crippling according to the AISI Specification for the Design of Cold-Formed Steel Structural Members [9].

All beam tests were performed in the MTS 880 Test System located in the Engineering Research Laboratory at the University of Missouri-Rolla. The "stroke" (actuator displacement) was used as the control mode to maintain a constant actuator speed for flexural beam tests. This test system consisted of an MTS load frame, a control console, and the CAMAC (Computer Automated Measurement and Control) data acquisition system. The data acquisition used in this study consisted of 64 simultaneously sampling input channels at a resolution of 12 bits. The test frequency or sampling rate depended on the total test time with a maximum of 25,000 readings per second for each channel.

All specimens were cold formed by a press-brake operation with a nominal inside-bend radius of 5/32 inch. A total of 72 hat-shaped beams were tested to study the effect of strain rate on the local buckling and post-buckling strengths of compression elements. Three selected strain rates (10^{-4}, 10^{-3}, and 10^{-2} in./in./sec.) were used in the beam tests. As shown in Figure 2.2, four groups of test specimens were used in this investigation:

- Group W - hat-shaped beams which were assembled by using a hat section fabricated from 25AK sheet steel and a plate of 50SK sheet steel. The stiffened flange of the hat section was in compression.
- Group Z - hat-shaped beams which were assembled by using a hat section fabricated from 25AK sheet steel and a plate of 50SK sheet steel. The stiffened flange of the hat section was in tension.
- Group S - hat-shaped beams which were assembled by using a hat section fabricated from 50SK sheet steel and a plate of 25AK sheet steel. The stiffened flange of the hat section was in compression.
- Group K - hat-shaped beams which were assembled by using a hat section fabricated from 50SK sheet steel and a plate of 25AK sheet steel. The stiffened flange of the hat section was in tension.

Tables 2.4 through 2.7 give the lengths and dimensions of beam specimens fabricated from 25AK and 50SK sheet steels. For the specimens with the stiffened flange of hat sections on the compression side, the w/t ratios of stiffened flanges ranged from 9.26 to 63.33 and from 24.78 to 69.70 for Group W and Group S, respectively. For the specimens with the plate on the compression side, the w/t ratios of plates ranged from 25.61 to 82.49 and from 37.09 to 79.46 for Group Z and Group K, respectively.

Six foil strain gages were used to measure strains at the midspan of beams for the specimens with small w/t ratios. The locations of strain gages, numbered from 1 to 6, are

shown in Figure 2.3. For the beam specimens with medium and large w/t ratios, additional four strain gages were mounted along the longitudinal centerline of stiffened flanges (Groups W and S) and stiffened plates (Groups Z and K). These two paired strain gages were placed at a distance equal to the overall width of the stiffened compression flange of hat sections (Groups W and S) or the stiffened compression plates (Groups Z and K).

The paired strain gages placed along the centerline of compression elements of beams were used to determine the tested local bucking load by means of the modified strain reversal method, which is discussed in Reference 10. The strain gages placed along two sides of compression and tension elements at the midspan of beams were used to measure the tested yield and maximum strains of specimens.

The beam specimen was simply supported and the load was applied from the lower compression platen to the specimen. C-shaped clamps were used in the tests to clamp both sides of beam specimens to 4-inch wide bearing plates. Two LVDT (Linear Variable Differential Transformer) were used at midspan to measure the beam deflections and to check any rotation of beam specimens during the test. The applied load, actuator displacement, strains from 10 strain gage output, and the deflections from two LVDT outputs were recorded and stored in the CAMAC memory. After the data were acquired, it was download to the computer for analysis purpose.

It was found that the critical local buckling moment, yield moment, and ultimate moment of hybrid beams increase with increasing strain rate for specimens having the similar w/t ratios for most cases. The failure mode of the beam specimen varies with the width-to-thickness ratio of the compression stiffened flange (Groups W and S) and stiffened plate (Groups Z and K). The tested critical local buckling moment, yield moment, and ultimate moment for each specimen are evaluated and presented in the Twentieth Progress Report [4].

III. Evaluation of Experimental Data

A. GENERAL

In the previous phase of study [4], a total of 72 hat-shaped hybrid beams, fabricated from 25AK and 50SK sheet steels were tested under different strain rates to study the behavior of stiffened compression elements. It was concluded that the predicted critical local buckling moment, yield moment, and ultimate moment of hybrid beams can be improved by using dynamic yield stresses. Since the yield strength and stress-strain relationship of the two materials used to fabricate the beam specimens are different, the yield moment of hybrid beams can not be easily computed. Therefore, the present phase of the research is to develop an alternative procedure by using transformed sections, which may be utilized in the calculation of load-carrying capacity of cold-formed steel hybrid beams.

All beam specimens were subjected to pure moments between two loading points located at one-fourth of span length from end supports. The weight of test beam specimen and the cross beam placed on the top of the specimen are light enough (approximate 80 lbs.) to be neglected in the evaluation of most test results. In some cases, it is necessary to consider the effect of the weight of test specimen and cross beam in the evalution due to the initial loading and deflection. The dynamic tensile and compressive yield stresses obtained from material tests were used for calculating the yield moment (M_y).

B. YIELD MOMENTS

a. Conventional Method Using Effective Design Width Formulas. According to the AISI Specification [9], two procedures can be used to calculate the section strength of beams. One is based on the initiation of yielding using the effective section and the other is based on the inelastic reserve capacity. In this report, it is assumed that the beam reaches its yield moment when the maximum edge stress in the extreme fiber reaches the yield stress of steel. In addition, the compression elements of thin-walled structural members with relatively large w/t ratios can continue to carry additional loads after the attainment of elastic buckling. However, the stresses in the compression elements will redistribute to develop the postbuckling strength. Therefore, the concept of the effective width design can be used to calculate the effective section properties. According to the AISI Automotive Steel Design Manual [1], the effective design width of compression elements can be used for determining the load-carrying capacity of the member when the slenderness factor λ computed according to Equation 3.1 exceeds a value of 0.673.

$$\lambda = 1.052\left[\frac{w}{t}\right]\frac{\sqrt{f}}{\sqrt{k}\sqrt{E}} \tag{3.1}$$

where f = stress in the element

E = modulus of elasticity of the steel, 29500 ksi

k = buckling coefficient for the flat plate

w = flat width of the element

t = thickness of the element

when $\lambda = 0.673$, the limiting width-to-thickness ratio (at which full capacity is achievable) can be evaluated as

$$\left[\frac{w}{t}\right]_{\lim} = 0.64\sqrt{\frac{kE}{f}} \tag{3.2}$$

For fully stiffened compression elements under a uniform stress, k = 4, which gives a limiting w/t value as follows [1]:

$$\left[\frac{w}{t}\right]_{\lim} = S = 1.28\sqrt{\frac{E}{f}} \tag{3.3}$$

For w/t exceeding the values of S, the effective width, b, is less than the actual width w. For the purpose of calculating sectional properties, the effective width is divided into two parts and each half is positioned adjacent to each longitudinal support. Thus the width (w-b) is considered to be removed at the center of the flat width when evaluating the sectional properties. The effective width b can be calculated from the 1996 AISI Automotive Steel Design Manual [1] as given in Equation 3.4:

$$b = w\left[\frac{1-\frac{0.22}{\lambda}}{\lambda}\right] \tag{3.4}$$

Based on the initiation of yielding, the computed yield moment ($(M_y)_{comp}$) of a homogeneous beam can be calculated by using the following equation:

$$(M_y)_{comp} = F_y S_e \tag{3.5}$$

where F_y = yield stress of steel

S_e = elastic section modulus of effective section

b. Alternative Procedure Using Transformed Section. Equation 3.5 may not apply directly to the hybrid beam fabricated from two different sheet steels because it is based on the assumption that the beam is homogeneous. For the case of hybrid beams fabricated from both sharp-yielding type of sheet steels, Equation 3.5 could be used to calculate the yield moment if the element fabricated from the sheet steel with a lower yield strength reaches the yield point first. The 20th Progress Report illustrates the calculation of M_y for hybrid beam using two sheet steels having different stress-strain curves.

To deal with the hybrid beam, the alternative procedure presented herein is to transform the built-up section consisting of different steels into an equivalent homogeneous beam. Because the tested beam specimens used in this phase of study consisted of four groups (Groups W, Z, S, and K) which were fabricated from two different sheet steels with different stress-strain curves, the structural strength of these hybrid beams can be calculated by using the transformed section concept. As can be seen in Figure 3.1, the cross-sectional area of the plate fabricated from 50SK sheet steel (A_{50SK}) can be transformed to

the equivalent area of 25AK sheet steel by using nA_{50SK} for Groups W and Z specimens. Similarly, for S and K specimens, the cross-sectional area of the plate fabricated from 25AK sheet steel (A_{25AK}) can be transformed to the equivalent area of 50SK sheet steel by using $(1/n)A_{25AK}$. The variable "n" is denoted as the ratio of the secant moduli given in Equation 3.6.

$$n = \frac{E_{50SK}}{E_{25AK}} \tag{3.6}$$

Where E_{50SK} and E_{25AK} are the secant moduli for 50SK and 25AK sheet steels, respectively.

Based on the transformed section method, the yield moment of the hybrid beam can be estimated by assuming that the strain of the plane section in the beam varies directly with the distance from the neutral axis. The variable of n used in this investigation can be computed by using the constants, n_1 and n_2, based on the mechanical properties of these two sheet steels. The values of these two constants are listed in Equations 3.7 and 3.8. Figures 3.2 and 3.3 show comparisons of typical stress-strain relationships for 25AK sheet steel subjected to longitudinal tension and compression under four strain rates of 10^{-4}, 10^{-2}, 10^{-1}, and 1.0 in./in./sec.. The typical stress-strain relationships for 50SK sheet steel under tension and compression are shown in Figures 3.4 and 3.5.

$$n1 = \frac{(\frac{\sigma_{pr}}{\varepsilon_{pr}})_{50SK}}{(\frac{\sigma_{pr}}{\varepsilon_{pr}})_{25AK}} = 1.05 \tag{3.7}$$

$$n2 = \frac{\left(\frac{\sigma_y}{\varepsilon_y}\right)_{50SK}}{\left(\frac{\sigma_y}{\varepsilon_y}\right)_{25AK}} = 2.39 \tag{3.8}$$

$$n = \frac{n1 + n2}{2} = 1.72 \tag{3.9}$$

where σ_{pr} = proportional limit of sheet steel

σ_y = yield stress of sheet steel

ε_{pr} = strain of proportional limit

ε_y = strain of yield stress

The proportional limits of 25AK and 50SK sheet steels were obtained by the offset method according to the AISI Commentary [11]. In the offset method, the proportional limit is the stress corresponding to the intersection of the stress-strain curve and a line parallel to the initial straight-line portion offset by a specified strain. The offset is usually specified as 0.01%. The yield strength of sharp-yielding sheet steel is determined by the stress where the stress-strain curve becomes horizontal. Therefore, the lower yield point of stress-strain diagram was used to determine the yield strength for 50SK sheet steel. For

the gradual-yielding type stress-strain curve (25AK sheet steel), the yield strength was determined by the intersection of the stress-strain curve and the straight line drawn parallel to the elastic portion of the stress-strain curve at an offset of 0.2 percent.

According to the test results which were based on the readings obtained from the strain gages mounted on the top and bottom sides of beam specimens, it was found that the ratio of secant moduli (n) may be used to locate the assumed neutral axis of the transformed cross section for the hybrid beam specimens fabricated from 25AK and 50SK sheet steels. Once the neutral axis was located, the computed yield moment of a beam corresponding to the initiation of yielding can be calculated by using the subsequent steps.

(a) For the case of initiation of yielding occurring in the top compression flange of the beam such as cases A, B, and C of Groups W and S, and case C of Group Z, the yield moment can be computed by the following steps:

1. The section is subdivided into a number of elements (a total of 12 segments were used in the calculation as shown in Figure 3.6).
2. A position of the trial neutral axis is locateded based on the transformed cross section and the strain in the top fiber of the compression flange is assumed to be the yield strain of the steel. Based on these two values, the average strains in various elements are calculated.
3. From the simulated stress-strain relationships discussed in the next section, the average stresses σ in various elements corresponding to such computed strains are found.

4. Calculate the effective width of the compression flange according to the yield stress of the steel in the compression flange.
5. Compute the area A, including the effective section of compression flange, for each element.
6. Locate the neutral axis of transformed section by iteration until $\Sigma \Delta A \sigma = 0$ is satisfied.
7. The computed yield moment of a hybrid beam can be calculated by multiplying the force ($\Delta A \sigma$) and the distance for each element and summing up these values ($\Sigma \Delta A \sigma y$), in which y is the distance measured from the neutral axis to the centroid of each element.

(b) For the case of initiation of yielding occurring in the bottom tension flange of the beam such as cases A, B, and C of Group K and cases A and B of Group Z, the computed yield moment can be obtained by using the same steps discussed previously for the initiation of yielding occurred in the top compression flange except that steps (2) and (4) are changed as follows:

2. A position of the trial neutral axis is locateded based on the transformed cross section and the strain in the bottom fiber of the tension flange is assumed to be the yield strain of the steel. Based on these two values, the average strains in various elements are calculated.

4. Calculate the effective width of the stiffened compression flange for the compression stress obtained from the yield strain of the steel in the tension flange and the assumed neutral axis.

It should be noted that for Groups Z and K specimens having stiffened compression plate, the effective width of the compression flange was calculated based on the actual thickness and width. The transformed section can be computed on the basis of the effective sectional area of the stiffened plate and cross-sectional area of the hat section.

c. Stress-Strain Relationship. The types of stress-strain relationship for 25AK and 50SK sheet steels are different. As can be seen in Figure 3.7, the stress-strain relationship for 25AK sheet steel is the gradual-yielding type, and it is the sharp-yielding type for 50SK sheet steel. The following empirical equations were derived from material tests and used to compute the stresses and strains for 25AK and 50SK sheet steels under different strain rates:

For 25AK sheet steel $\sigma = A + B/\varepsilon + C/\varepsilon^2$ (3.10)

For 50SK sheet steel $\sigma = D + E\times\varepsilon + F\times\varepsilon^2$ (3.11)

where σ = compressive stress, ksi

ε = compressive strain (%)

when strain rate = 10^{-4} in./in./sec.:

A = 23.67 B = -0.465 C = -0.024

D = 1.403 E = 334.7 F = -454.7

when strain rate = 10^{-3} in./in./sec.:

A = 24.25 B = -0.153 C = -0.028

D = 1.377 E = 331.7 F = -431.2

when strain rate = 10^{-2} in./in./sec.:

A = 24.84 B = 0.159 C = -0.053

D = 1.350 E = 328.6 F = -407.6

The strains used for determining the above equations were selected from the proportional limit to the yield point of steel. For the stresses below the proportional limit of the material, the following two empirical equations derived from material tests give the stress-strain relationships for 25AK and 50SK sheet steels:

For 25AK sheet steel $$\sigma = \frac{A}{B}\varepsilon \tag{3.12}$$

For 50SK sheet steel $$\sigma = \frac{C}{D}\varepsilon \tag{3.13}$$

where σ = compressive stress, ksi

ε = compressive strain expressed in percent

when strain rate = 10^{-4} in./in./sec.:

A = 15.94 B = 0.065

C = 41.97 D = 0.153

when strain rate = 10^{-3} in./in./sec.:

A = 17.73 B = 0.078

C = 42.23 D = 0.154

when strain rate = 10^{-2} in./in./sec.:

A = 19.51 B = 0.086

C = 42.49 D = 0.155

From practical point of view, by applying Equations 3.10 to 3.13 in the calculation of yield moment seems too complicated. Since the types of stress-strain relationships for these two sheet steels (25AK and 50SK) are different, the approximate stress-strain relationships as shown in Figure 3.8 were adopted to calculate the computed yield moments. As mentioned in the 20th Progress Report, by comparing the tested yield moments with the computed values calculated on the basis of the approximate stress-strain relationships for

Group W specimens, it was observed that the computed yield moment can not provide a good prediction. The use of approximate stress-strain relationships as given in Figure 3.8 would result in conservative predicted yield moments particularly for the beams with small w/t ratios. For details, refer to Reference 4.

In order to simplify the calculation procedure, the simulated stress-strain relationships were constructed as shown in Figure 3.9. For the stresses below the proportional limit of the material, Equation 3.14 can be used to represent the stress-strain relationships of sheet steels. Equation 3.15 expresses the stress-strain relationships for the stress level between the proportional limit and the yield point of steel.

$$\sigma = \frac{\sigma_{pr}}{\varepsilon_{pr}} \times \varepsilon \tag{3.14}$$

$$\sigma = \left(\sigma_y - \sigma_{pr}\right) \frac{\left(\varepsilon - \varepsilon_{pr}\right)}{\left(\varepsilon_y - \varepsilon_{pr}\right)} + \sigma_{pr} \tag{3.15}$$

d. Discussion. The yield moments can be computed by applying the transformed section method and simulated stress-strain relationships in the Alternative Procedure listed in Section III.b. The tested yield moments of beam specimens were determined from the product of bending arm (L/4) and one half of the yield load ($P_y/2$) as follows:

$$\left(M_y\right)_{test} = \frac{P_y L}{8} \tag{3.16}$$

The computed and tested yield moments are presented in Tables 3.1 and 3.2 for Groups W and Z specimens, for which the hat sections were fabricated from 25AK sheet steel and the plates were fabricated from 50SK sheet steel. Tables 3.3 and 3.4 are for Groups S and K specimens, for which the hat sections were fabricated from 50SK sheet steel and the plates were fabricated from 25AK sheet steel. The computed yield moments listed in column (4) of these tables are based on the dynamic compressive stresses corresponding to the strain rates used in the tests. It is noted from Tables 3.1 through 3.4 that the tested yield moment increases with increasing strain rate for specimens having the similar w/t ratios. Tables 3.5 through 3.8 present the similar data for Groups W, Z, S, and K specimens except that the computed yield moments were calculated based on the dynamic tensile stresses. The dynamic compressive and tensile stresses used in the calculation of computed yield moments were determined by using the simulated stress-strain relationships listed in Equations 3.14 and 3.15 for both 25AK and50SK sheet steels. The tested yield loads corresponding to the initiation of yielding are listed in column (3) of these tables, and the tested yield moments are listed in column (5) of these tables.

Comparisons of the computed and tested yield moments are listed in column (6) of these tables. By observing the values of $(M_y)_{test}/(M_y)_{comp}$ ratios, it can be seen that the difference between the tested and predicted yield moments is within 10 percent for most specimens. Therefore, the alternative procedure using transformed sections and simulated stress-strain curves seems to provide a good prediction for the yield moment of hybrid

beams fabricated from two different materials. It was also observed from Tables 3.1, 3.2, 3.5, and 3.6 that the values of $(M_y)_{test}/(M_y)_{comp}$ ratios are quite close for the same case of beam specimens having similar dimensions but tested under different strain rates. But for the Groups S and K specimens, it can be seen from Tables 3.3, 3.4, 3.7, and 3.8 that the values of $(M_y)_{test}/(M_y)_{comp}$ ratios slightly increase with increasing strain rates for the same case of beam specimens. This is because the strain rate sensitivity for 25AK and 50SK sheet steels are different. As can be seen in Figure 3.1, the cross-sectional area of stiffened plate fabricated from 25AK sheet steel is reduced and transformed to 50SK material for Groups S and K specimens. In fact, the strain rate sensitivity of 25AK sheet steel is higher than the strain rate sensitivity of 50SK sheet steel.

The ratios of tested-to-computed yield moments for case A of Groups W and Z are larger than the values for cases B and C. This is possibly due to the cold work of forming and the gradual yielding type of stress-strain curve for 25AK sheet steel. It is also noted that the ratios of tested-to-computed yield moments for all cases of Group K specimens are slightly less than the values for all cases of Group S, it is possibly due to the initial deformation of beam specimens which were caused by welding during the fabrication. The direction of initial deformation of entire beams is upward for Group S specimens and is downward for Group K specimens as mentioned in the 20th Progress Report [4].

According to Equation 3.5, the computed yield moment was determined on the basis

of the effective design width formulas (Equation 3.4) with the extreme compression or tension stress at yield point for homogeneous beams. Tables 3.9 and 3.10 list the computed and tested yield moments for Groups S and K specimens, for which the computed values were calculated by applying the transformed section in Equation 3.5. The computed yield moments listed in column (4) of these two tables are based on the dynamic compressive yield stresses corresponding to the strain rates used in the tests. The mean values of $(M_y)_{test}/(M_y)_{comp}$ ratios for Groups S and K specimens are 0.996 and 0.930 with standard deviations of 0.039 and 0.030, respectively. Tables 3.11 and 3.12 show the similar data for Groups S and K specimens except that the computed yield moments were obtained based on the dynamic tensile yield stresses. The mean values and standard deviations of $(M_y)_{test}/(M_y)_{comp}$ ratios are (0.978 and 0.041) for Group S specimens and (0.916 and 0.034) for Groups K specimens. However, Equation 3.5 gives unsatisfactory results for the calculation of yield moments of the W and Z specimens for which the sheet steel used for analyzing transformed sections is 25AK material. Since the stress-strain relationship for 25AK sheet steel is gradual-yielding type, it can be seen from Tables 3.13 and 3.14 for Groups W and Z specimens, respectively, that the use of Equation 3.5 would result in conservative predicted yield moments particularly for the beams with small w/t ratios.

A summary of ratios of tested to computed yield moments for both the calculating procedure discussed in this chapter and the procedure used in the 20th Progress Report are

presented in Table 3.15. It can seen that the alternative procedure using transformed sections and simulated stress-strain curves gives the similar results for the predicted yield moments computed by the procedure using the real stress-strain relationships presented in the 20th Progress Report.

The measured deflections under yield moments are between length/50 and length/100 for all tested specimens. It was observed from the tests that the deflection of the beam specimen under the ultimate load is quite large comparing with the deflection under yield load particularily for Groups Z and K specimens. Since the design procedures recommended in the AISI Design Manual [1] can not be used to compute the ultimate flexural strength for the specimens studied in this investigation, by using the reference strain obtained from the beam test and the same procedure presented in the 20th Progress Report, the ultimate moments were calculated. For more details, please refer to the 20th Progress Report.

IV. Conclusions

A total of 72 hat-shaped beams were studied in this phase of study. The materials used in the fabrication of hybrid beams were 25AK and 50SK sheet steels. Four groups of hat-shaped beams were tested under different strain rates. The transformed section concept and simulated stress-strain relationship were adopted in the calculation of yield moments for design purpose. Comparisons between the tested and computed values for yield moments were made in this report. The following conclusions can be drawn for the hybrid beams fabricated from 25AK and 50SK sheet steels:

- The differences between the tested and computed values for yield moments are within 10 percent for most specimens. It seems that the transformed section method could be used for the calculation of yield moment of hybrid beams.
- The calculation procedures presented in this report give reasonable results for yield moment of hybrid beams.
- Both dynamic compressive and tensile stresses can be used for calculating the yield moment of hybrid beams.
- It was found that the computed yield moments based on tensile stresses are less conservative than the computed values based on compressive stresses.

- The effective cross-sectional area determined according to AISI Design Manual [1] and AISI Specification [9] can also be employed in the calculation of yield moment for hybrid sections.
- The simulated stress-strain relationships can be used in the calculation of yield moment of hybrid beams for both 25AK and 50SK sheet steels.
- If the sheet steel used for analyzing transformed sections is a sharp-yielding type of stress-strain relationship, Equation 3.5 can be adopted for calculating yield moment of hybrid beams.

In summary, the effective design width formulas and the dynamic material properties can be used for the calculation of load-carrying capacity of hybrid beams. Using a transformed section method and applying the simulated stress-strain relationship, the calculation procedure discussed in Chapter III can provide a reasonable approach for computing the yield moment of hybrid beams. For sheet steels used in practical design without the tested stress-strain relationships, the AISI formulas (Equation 3.5) can be applied for calculating the yield moment of hybrid beams, when the sheet steel used for analyzing the transformed section has a sharp-yielding type of stress-strain relationship. As can be seen in Tables 3.13 and 3.14, Equation 3.5 may also be used for computing the yield moment of hybrid beams with medium and large w/t ratios, when the sheet steel used for analyzing the transformed section has a gradual-yielding type of stress-strain curve, however, the use of Equation 3.5 could result in a conservative predicted yield moment particularly for the compact beams with small w/t ratios.

For the case of hybrid beams fabricated from both sharp-yielding type of sheet steels, Equation 3.5 (AISI formulas) could be used to calculate the yield moment if the element fabricated from the sheet steel with a lower yield strength reaches the yield point first. For other cases such as the hybrid beam fabricated from two different sheet steels with different stress-strain curves, it seems that the procedure for calculating the yield moment of hybrid beam can be simplify by using transformed-section concept. The suggested flow chart of calculating the hybrid hat-shaped beams is shown in Figure 3.10. Future study can be used to verify and improve the findings.

Acknowledgments

The research work reported herein was conducted in the Department of Civil Engineering at the University of Missouri-Rolla under the sponsorship of the American Iron and Steel Institute.

The financial assistance granted by the Institute and the technical guidance provided by members of the AISI Task Force on Automotive Structural Design of the AISI Automotive Applications Committee and the AISI staff (S.J. Errera and D.C. Martin) are gratefully acknowledged. Members of the Task Force are: Messrs. G.A. Beecher, J. Borchelt, T. Kahlil, R.W. Lautensleger, H.F. Mahmood, D. Malen, E.C. Oren (chairperson), M.Y. Sheh, and M.T. Vecchio. Former members of the Task Force included Messrs. C. Haddad, C.M. Kim, J.G. Schroth, and T.N. Seel.

All materials used in the experimental study were donated by Inland Steel Company and National Steel Corporation.

References

1. American Iron and Steel Institute, "Automotive Steel Design Manual," Revision 5, May, 1996.
2. Pan, C.L. and Yu, W.W., "Influence of Strain Rate on the Structural Strength of Cold-Formed Steel Automotive Components," Proceedings of International Body Engineering Conference, edited by M. Nasim Uddin, September, 1993.
3. Kassar, M. and Yu, W.W., "Design of Automotive Structural Components Using High Strength Sheet Steels: Effect of Strain Rate on Material Properties of Sheet Steels and Structural Strengths of Cold-Formed Steel Members," Fourteenth Progress Report, Civil Engineering Study 90-2, University of Missouri-Rolla, May, 1990.
4. Pan, C.L. and Yu, W.W., "Design of Automotive Structural Components Using High Strength Sheet Steels: Effect of Strain Rate on the Structural Strength of Cold-Formed Steel Hybrid Beams," Twentieth Progress Report, Civil Engineering Study 95-1, University of Missouri-Rolla, Dec., 1995.
5. Frost, R.W. and Schilling, C.G., "Behavior of Hybrid Beams Subjected to Static Loads," Journal of Structural Division, Proceedings of the American Society of Civil Engineers, Vol. 90, No. ST3, 1964.
6. Pan, C.L. and Yu, W.W., "Design of Automotive Structural Components Using High Strength Sheet Steels: Mechanical Properties of Materials," Seventeenth Progress Report, Civil Engineering Study 92-2, University of Missouri-Rolla, May, 1992.

7. Pan, C.L. and Yu, W.W., "Design of Automotive Structural Components Using High Strength Sheet Steels: Influence of Strain Rate on the Mechanical Properties of Sheet Steels and Structural Performance of Cold-Formed Steel Members," Eighteenth Progress Report, Civil Engineering Study 92-3, University of Missouri-Rolla, Dec., 1992.
8. Pan, C.L. and Yu, W.W., Schell, B.C., and Sheh, M.Y., "Effect of Strain Rate on the Structural Strength and Crushing Behavior of Hybrid Stub Columns," Proceedings of International Body Engineering Conference, edited by M. Nasim Uddin, September, 1994.
9. American Iron and Steel Institute, "Specification for the Design of Cold-Formed Steel Structural Members," Cold-Formed Steel Design Manual, Part I, 1986 Edition with the 1989 Addendum.
10. Johnson, A.L. and Winter, G., "The Structural Performance of Austenitic Stainless Steel Members," Report No. 327, Cornell University, Nov. 1966.
11. American Iron and Steel Institute, "Commentary for the Design of Cold-Formed Steel Structural Members," Cold-Formed Steel Design Manual, Part II, 1986 Edition with the 1989 Addendum.

Table 2.1

Average Mechanical Properties of 25AK Sheet Steel Used in the Experimental Study under Different Strain Rates

Strain Rate in./in./sec.	$(F_y)_c$ (ksi)	$(F_{pr})_c$ (ksi)	$(F_y)_t$ (ksi)	$(F_u)_t$ (ksi)	Elongation (%)
0.0001	21.66	15.93	24.60	42.76	-----
0.01	24.77	19.55	27.86	44.44	49.31
0.1	29.80	22.81	31.72	47.35	50.98
1.0	38.14	*****	35.13	51.25	58.18

Table 2.2

Average Mechanical Properties of 50SK Sheet Steel Used in the Experimental Study under Different Strain Rates

Strain Rate in./in./sec.	$(F_y)_c$ (ksi)	$(F_{pr})_c$ (ksi)	$(F_y)_t$ (ksi)	$(F_u)_t$ (ksi)	Elongation (%)
0.0001	53.35	41.98	54.97	67.07	36.09
0.01	55.91	42.46	56.83	68.98	33.34
0.1	56.96	44.36	58.06	71.04	34.45
1.0	59.41	*****	60.73	76.50	40.13

Note: (1) $(F_y)_c$ and $(F_{pr})_c$ are based on longitudinal compression coupon tests.

(2) $(F_y)_t$, $(F_u)_t$ and Elongation are determined from longitudinal tension coupon tests.

(3) Elongation was measured by using a 2-inch gage length.

Table 2.3

Designation of Beam Specimens Used in This Study

1st Digit	1st Letter	2nd Digit	2nd Letter	3rd Letter
Test Type	w/t Ratio (Case)	Strain-Rate (in./in./sec.)	Test No.	Section Type (Group)
3: Beam Test	A: Small	1: 0.0001	A: 1st Test	W: Hat Sec.-25AK Plate -50SK
	B: Medium	2: 0.001	B: 2nd Test	Z: Hat Sec.-25AK Plate -50SK
	C: Large	3: 0.01		S: Hat Sec. -50SK Plate -25AK
				K: Hat Sec. -50SK Plate -25AK

Note: (1) For the specimens with the section types of "W" or "S", the stiffened plates were tested on the tension side.

(2) For the specimens with the section types of "Z" or "K", the stiffened plates were tested on the compression side.

(3) See Figure 2.2.

Table 2.4

Dimensions of Group W Beam Specimens

(a) Dimensions of Hat Sections (25AK Sheet Steel)

Spec.	BF (in.)	BW (in.)	BL (in.)	t (in.)	w/t	Length (in.)
3A1AW	1.196	1.088	0.904	0.078	9.33	35.0
3A1BW	1.191	1.090	0.901	0.078	9.26	35.0
3A2AW	1.198	1.087	0.904	0.078	9.35	35.0
3A2BW	1.220	1.069	0.898	0.078	9.63	35.0
3A3AW	1.194	1.093	0.893	0.078	9.30	35.0
3A3BW	1.210	1.083	0.895	0.078	9.51	35.0
3B1AW	2.696	1.577	0.888	0.078	28.56	60.0
3B1BW	2.707	1.577	0.911	0.078	28.70	60.0
3B2AW	2.709	1.580	0.912	0.078	28.72	60.0
3B2BW	2.717	1.577	0.910	0.078	28.83	60.0
3B3AW	2.699	1.574	0.905	0.078	28.60	60.0
3B3BW	2.701	1.573	0.903	0.078	28.62	60.0
3C1AW	5.404	2.061	0.911	0.078	63.28	72.0
3C1BW	5.405	2.064	0.903	0.078	63.29	72.0
3C2AW	5.402	2.068	0.912	0.078	63.25	72.0
3C2BW	5.399	2.059	0.915	0.078	63.21	72.0
3C3AW	5.406	2.052	0.903	0.078	63.30	72.0
3C3BW	5.408	2.051	0.906	0.078	63.33	72.0

Note: (1) For symbols of dimensions, see Figure 2.1.

(2) The inside bending radius is 0.15625 (5/32) inch.

Table 2.4 (cont'd)
Dimensions of Group W Beam Specimens
(b) Dimensions of Plate Sections (50SK Sheet Steel)

Spec.	BP (in.)	t (in.)	w/t	Length (in.)
3A1AW	2.796	0.074	25.57	35.0
3A1BW	2.798	0.074	25.64	35.0
3A2AW	2.795	0.074	25.55	35.0
3A2BW	2.791	0.074	25.58	35.0
3A3AW	2.794	0.074	25.69	35.0
3A3BW	2.801	0.074	25.76	35.0
3B1AW	4.297	0.074	46.07	60.0
3B1BW	4.297	0.074	45.76	60.0
3B2AW	4.311	0.074	45.93	60.0
3B2BW	4.327	0.074	45.18	60.0
3B3AW	4.296	0.074	45.82	60.0
3B3BW	4.302	0.074	45.93	60.0
3C1AW	7.010	0.074	82.42	72.0
3C1BW	7.003	0.074	82.43	72.0
3C2AW	7.006	0.074	82.35	72.0
3C2BW	7.001	0.074	82.24	72.0
3C3AW	7.005	0.074	82.46	72.0
3C3BW	7.003	0.074	82.39	72.0

Note: For symbols of dimensions, see Figure 2.1.

Table 2.5

Dimensions of Group Z Beam Specimens

(a) Dimensions of Hat Sections (25AK Sheet Steel)

Spec.	BF (in.)	BW (in.)	BL (in.)	t (in.)	w/t	Length (in.)
3A1AZ	1.194	1.092	0.900	0.078	9.30	35.0
3A1BZ	1.191	1.092	0.903	0.078	9.26	35.0
3A2AZ	1.193	1.091	0.931	0.078	9.29	35.0
3A2BZ	1.199	1.088	0.900	0.078	9.37	35.0
3A3AZ	1.212	1.079	0.901	0.078	9.53	35.0
3A3BZ	1.195	1.090	0.898	0.078	9.31	35.0
3B1AZ	2.690	1.589	0.900	0.078	28.48	60.0
3B1BZ	2.701	1.579	0.903	0.078	28.62	60.0
3B2AZ	2.704	1.577	0.910	0.078	28.66	60.0
3B2BZ	2.694	1.582	0.906	0.078	28.53	60.0
3B3AZ	2.703	1.575	0.918	0.078	28.65	60.0
3B3BZ	2.699	1.578	0.910	0.078	28.60	60.0
3C1AZ	5.405	2.058	0.909	0.078	63.29	72.0
3C1BZ	5.403	2.071	0.907	0.078	63.26	72.0
3C2AZ	5.401	2.068	0.903	0.078	63.24	72.0
3C2BZ	5.396	2.062	0.907	0.078	63.17	72.0
3C3AZ	5.403	2.057	0.906	0.078	63.26	72.0
3C3BZ	5.401	2.058	0.908	0.078	63.24	72.0

Note: (1) For symbols of dimensions, see Figure 2.1.

(2) The inside bending radius is 0.15625 (5/32) inch.

Table 2.5 (cont'd)
Dimensions of Group Z Beam Specimens
(b) Dimensions of Plate Sections (50SK Sheet Steel)

Spec.	BP (in.)	t (in.)	w/t	Length (in.)
3A1AZ	2.796	0.074	25.62	35.0
3A1BZ	2.798	0.074	25.61	35.0
3A2AZ	2.805	0.074	25.73	35.0
3A2BZ	2.799	0.074	25.66	35.0
3A3AZ	2.799	0.074	25.65	35.0
3A3BZ	2.803	0.074	25.74	35.0
3B1AZ	4.300	0.074	45.95	60.0
3B1BZ	4.299	0.074	45.89	60.0
3B2AZ	4.294	0.074	45.73	60.0
3B2BZ	4.297	0.074	45.82	60.0
3B3AZ	4.302	0.074	45.73	60.0
3B3BZ	4.298	0.074	45.78	60.0
3C1AZ	7.001	0.074	82.32	72.0
3C1BZ	7.003	0.074	82.38	72.0
3C2AZ	7.007	0.074	82.49	72.0
3C2BZ	6.983	0.074	82.11	72.0
3C3AZ	7.004	0.074	82.41	72.0
3C3BZ	7.002	0.074	82.35	72.0

Note: (1) For symbols of dimensions, see Figure 2.1.

Table 2.6

Dimensions of Group S Beam Specimens

(a) Dimensions of Hat Sections (50SK Sheet Steel)

Spec.	BF (in.)	BW (in.)	BL (in.)	t (in.)	w/t	Length (in.)
3A1AS	2.298	1.045	0.781	0.074	24.83	50.0
3A1BS	2.302	1.042	0.797	0.074	24.89	50.0
3A2AS	2.304	1.049	0.792	0.074	24.91	50.0
3A2BS	2.298	1.045	0.807	0.074	24.83	50.0
3A3AS	2.308	1.047	0.794	0.074	24.97	50.0
3A3BS	2.294	1.043	0.797	0.074	24.78	50.0
3B1AS	3.591	1.560	0.794	0.074	42.30	65.0
3B1BS	3.608	1.540	0.801	0.074	42.53	65.0
3B2AS	3.602	1.541	0.805	0.074	42.45	65.0
3B2BS	3.586	1.549	0.813	0.074	42.24	65.0
3B3AS	3.603	1.545	0.808	0.074	42.47	65.0
3B3BS	3.305	1.546	0.803	0.074	42.49	65.0
3C1AS	5.607	2.047	0.804	0.074	69.55	72.0
3C1BS	5.611	2.036	0.807	0.074	69.60	72.0
3C2AS	5.609	2.053	0.807	0.074	69.57	72.0
3C2BS	5.618	2.050	0.812	0.074	69.70	72.0
3C3AS	5.588	2.019	0.810	0.074	69.29	72.0
3C3BS	5.605	2.045	0.804	0.074	69.52	72.0

Note: (1) For symbols of dimensions, see Figure 2.1.

(2) The inside bending radius is 0.15625 (5/32) inch.

Table 2.6 (cont'd)
Dimensions of Group S Beam Specimens
(b) Dimensions of Plate Sections (25AK Sheet Steel)

Spec.	BP (in.)	t (in.)	w/t	Length (in.)
3A1AS	3.706	0.078	37.50	50.0
3A1BS	3.703	0.078	37.26	50.0
3A2AS	3.706	0.078	37.36	50.0
3A2BS	3.704	0.078	37.14	50.0
3A3AS	3.704	0.078	37.31	50.0
3A3BS	3.706	0.078	37.29	50.0
3B1AS	5.001	0.078	53.94	65.0
3B1BS	4.997	0.078	53.79	65.0
3B2AS	5.003	0.078	53.82	65.0
3B2BS	5.004	0.078	53.73	65.0
3B3AS	5.003	0.078	53.78	65.0
3B3BS	5.001	0.078	53.82	65.0
3C1AS	7.000	0.078	79.44	72.0
3C1BS	6.999	0.078	79.38	72.0
3C2AS	7.004	0.078	79.45	72.0
3C2BS	7.007	0.078	79.38	72.0
3C3AS	6.998	0.078	79.33	72.0
3C3BS	7.001	0.078	79.45	72.0

Note: (1) For symbols of dimensions, see Figure 2.1.

Table 2.7

Dimensions of Group K Beam Specimens

(a) Dimensions of Hat Sections (50SK Sheet Steel)

Spec.	BF (in.)	BW (in.)	BL (in.)	t (in.)	w/t	Length (in.)
3A1AK	2.307	1.034	0.798	0.074	24.95	50.0
3A1BK	2.293	1.046	0.796	0.074	24.76	50.0
3A2AK	2.302	1.042	0.794	0.074	24.89	50.0
3A2BK	2.286	1.051	0.805	0.074	24.67	50.0
3A3AK	2.300	1.049	0.794	0.074	24.86	50.0
3A3BK	2.298	1.045	0.797	0.074	24.83	50.0
3B1AK	3.593	1.546	0.805	0.074	42.33	65.0
3B1BK	3.588	1.551	0.804	0.074	24.26	65.0
3B2AK	3.589	1.535	0.803	0.074	42.28	65.0
3B2BK	3.579	1.545	0.803	0.074	42.14	65.0
3B3AK	3.600	1.535	0.798	0.074	42.43	65.0
3B3BK	3.598	1.537	0.800	0.074	42.40	65.0
3C1AK	5.592	2.045	0.808	0.074	69.34	72.0
3C1BK	5.606	2.048	0.809	0.074	69.53	72.0
3C2AK	5.589	2.054	0.814	0.074	69.30	72.0
3C2BK	5.606	2.049	0.806	0.074	69.53	72.0
3C3AK	5.617	2.038	0.803	0.074	69.68	72.0
3C3BK	5.611	2.041	0.803	0.074	69.60	72.0

Note: (1) For symbols of dimensions, see Figure 2.1.

(2) The inside bending radius is 0.15625 (5/32) inch.

Table 2.7 (cont'd)
Dimensions of Group K Beam Specimens
(b) Dimensions of Plate Sections (25AK Sheet Steel)

Spec.	BP (in.)	t (in.)	w/t	Length (in.)
3A1AK	3.701	0.078	37.22	50.0
3A1BK	3.698	0.078	37.21	50.0
3A2AK	3.702	0.078	37.28	50.0
3A2BK	3.698	0.078	37.09	50.0
3A3AK	3.703	0.078	37.30	50.0
3A3BK	3.699	0.078	37.21	50.0
3B1AK	4.997	0.078	53.47	65.0
3B1BK	5.001	0.078	53.81	65.0
3B2AK	4.995	0.078	53.74	65.0
3B2BK	4.995	0.078	53.74	65.0
3B3AK	4.991	0.078	53.76	65.0
3B3BK	4.998	0.078	53.82	65.0
3C1AK	7.003	0.078	79.42	72.0
3C1BK	7.002	0.078	79.40	72.0
3C2AK	6.998	0.078	79.28	72.0
3C2BK	7.004	0.078	79.46	72.0
3C3AK	7.000	0.078	79.45	72.0
3C3BK	7.001	0.078	79.46	72.0

Note: (1) For symbols of dimensions, see Figure 2.1.

Table 3.1

Comparison of Computed and Tested Yield Moments
Beam Specimens - Group W
(Based on dynamic compressive stresses and a transformed tension flange, calculated by using alternative procedure)

Spec.	w/t (25AK) (1)	F_y (ksi) (2)	$(P_y)_{test}$ (kips) (3)	$(M_y)_{comp}$ (in.-kips) (4)	$(M_y)_{test}$ (in.-kips) (5)	(5)/(4) (6)
3A1AW	9.23	21.63	1.082	3.23	4.19	1.296
3A1BW	9.26	21.63	1.117	3.23	4.33	1.339
3A2AW	9.35	23.17	1.130	3.47	4.38	1.262
3A2BW	9.63	23.17	1.135	3.42	4.40	1.285
3A3AW	9.30	24.71	1.241	3.78	4.81	1.274
3A3BW	9.51	24.71	1.264	3.75	4.90	1.305
3B1AW	28.56	21.63	1.507	9.71	10.99	1.131
3B1BW	28.70	21.63	1.531	9.74	10.72	1.101
3B2AW	28.72	23.17	1.650	10.41	11.55	1.109
3B2BW	28.83	23.17	1.583	10.41	11.08	1.064
3B3AW	28.60	24.71	1.766	11.15	12.36	1.108
3B3BW	28.62	24.71	1.785	11.15	12.49	1.120
3C1AW	63.28	21.63	2.432	20.66	20.67	1.000
3C1BW	63.29	21.63	2.450	20.71	20.83	1.006
3C2AW	63.25	23.17	2.677	21.83	22.75	1.042
3C2BW	63.21	23.17	2.648	21.69	22.51	1.037
3C3AW	63.30	24.71	2.789	22.91	23.71	1.035
3C3BW	36.33	24.71	2.731	22.90	23.21	1.014
Mean						1.140
Standard Deviation						0.119

Note: The simulated stress-strain relationships of 25AK sheet steel as shown in Fig. 3.9 were used for calculating the yield moments ($(M_y)_{comp}$).

Table 3.2

Comparison of Computed and Tested Yield Moments
Beam Specimens - Group Z
(Based on dynamic compressive stresses and a transformed compression flange, calculated by using alternative procedure)

Spec.	w/t (25AK) (1)	F_y (ksi) (2)	$(P_y)_{test}$ (kips) (3)	$(M_y)_{comp}$ (in.-kips) (4)	$(M_y)_{test}$ (in.-kips) (5)	(5)/(4) (6)
3A1AZ	25.62	53.30	1.070	3.25	4.14	1.275
3A1BZ	25.61	53.30	1.111	3.24	4.31	1.329
3A2AZ	25.73	54.61	1.180	3.48	4.57	1.314
3A2BZ	25.66	54.61	1.164	3.48	4.51	1.297
3A3AZ	25.65	55.92	1.238	3.74	4.80	1.285
3A3BZ	25.74	55.92	1.278	3.76	4.95	1.316
3B1AZ	45.95	53.30	1.492	9.80	10.44	1.065
3B1BZ	45.89	53.30	1.550	9.74	10.85	1.113
3B2AZ	45.73	54.61	1.605	10.47	11.24	1.073
3B2BZ	45.82	54.61	1.611	10.39	11.27	1.085
3B3AZ	45.73	55.92	1.728	11.17	12.10	1.083
3B3BZ	45.78	55.92	1.680	11.19	11.76	1.051
3C1AZ	82.32	53.30	2.800	23.35	23.80	1.019
3C1BZ	82.38	53.30	2.870	23.55	24.40	1.036
3C2AZ	82.49	54.61	3.012	25.11	25.60	1.019
3C2BZ	82.11	54.61	3.060	24.99	26.01	1.040
3C3AZ	82.41	55.92	3.158	26.70	26.84	1.005
3C3BZ	82.35	55.92	3.140	26.71	26.69	0.999
Mean						1.133
Standard Deviation						0.127

Note: The simulated stress-strain relationships of 25AK sheet steel as shown in Fig. 3.9 were used for calculating the yield moments ($(M_y)_{comp}$).

Table 3.3

Comparison of Computed and Tested Yield Moments
Beam Specimens - Group S
(Based on dynamic compressive stresses and a transformed tension flange, calculated by using alternative procedure)

Spec.	w/t (25AK) (1)	F_y (ksi) (2)	$(P_{y)test}$ (kips) (3)	$(M_y)_{comp}$ (in.-kips) (4)	$(M_y)_{test}$ (in.-kips) (5)	(5)/(4) (6)
3A1AS	24.83	53.30	1.590	9.77	9.14	0.936
3A1BS	24.89	53.30	1.613	9.75	9.27	0.951
3A2AS	24.91	54.61	1.650	10.08	9.49	0.941
3A2BS	24.83	54.61	1.645	10.01	9.46	0.945
3A3AS	24.97	55.92	1.686	10.31	9.69	0.939
3A3BS	24.78	55.92	1.739	10.21	10.00	0.979
3B1AS	42.30	53.30	2.617	20.30	19.95	0.983
3B1BS	42.53	53.30	2.610	20.00	19.90	0.995
3B2AS	42.45	54.61	2.752	20.39	20.98	1.029
3B2BS	42.24	54.61	2.741	20.50	20.90	1.019
3B3AS	42.47	55.92	2.798	20.83	21.33	1.024
3B3BS	42.49	55.92	2.875	20.84	21.92	1.052
3C1AS	69.55	53.30	3.425	31.20	29.11	0.933
3C1BS	69.60	53.30	3.371	31.00	28.65	0.924
3C2AS	69.57	54.61	3.620	31.90	30.77	0.965
3C2BS	69.70	54.61	3.582	31.85	30.45	0.956
3C3AS	69.29	55.92	3.653	31.78	31.05	0.977
3C3BS	69.52	55.92	3.599	32.30	30.59	0.947
Mean						0.972
Standard Deviation						0.038

Note: The simulated stress-strain relationships of 50SK sheet steel as shown in Fig. 3.9 were used for calculating the yield moments ($(M_y)_{comp}$).

Table 3.4

Comparison of Computed and Tested Yield Moments
Beam Specimens - Group K
(Based on dynamic compressive stresses and a transformed compression flange, calculated by using alternative procedure)

Spec.	w/t (25AK) (1)	F_y (ksi) (2)	(P_y)test (kips) (3)	$(M_y)_{comp}$ (in.-kips) (4)	$(M_y)_{test}$ (in.-kips) (5)	(5)/(4) (6)
3A1AK	37.22	21.63	1.540	9.67	8.86	0.916
3A1BK	37.21	21.63	1.532	9.72	8.81	0.902
3A2AK	37.28	23.17	1.590	9.99	9.14	0.915
3A2BK	37.09	23.17	1.610	10.04	9.26	0.923
3A3AK	37.30	24.71	1.692	10.31	9.73	0.944
3A3BK	37.21	24.71	1.670	10.25	9.60	0.940
3B1AK	53.47	21.63	2.630	23.06	20.05	0.870
3B1BK	53.81	21.63	2.615	23.12	19.94	0.862
3B2AK	53.74	23.17	2.700	23.30	20.59	0.884
3B2BK	53.74	23.17	2.714	23.43	20.69	0.883
3B3AK	53.76	24.71	2.758	23.82	21.03	0.883
3B3BK	53.82	24.71	2.816	23.85	21.47	0.900
3C1AK	79.42	21.63	3.987	39.23	33.90	0.864
3C1BK	79.40	21.63	4.052	39.33	34.44	0.876
3C2AK	79.28	23.17	4.172	40.42	35.46	0.877
3C2BK	79.46	13.17	4.203	40.21	35.73	0.889
3C3AK	79.45	24.71	4.298	41.40	36.53	0.882
3C3BK	79.46	24.71	4.301	41.46	36.56	0.882
Mean						0.894
Standard Deviation						0.025

Note: The simulated stress-strain relationships of 50SK sheet steel as shown in Fig. 3.9 were used for calculating the yield moments ($(M_y)_{comp}$).

Table 3.5

Comparison of Computed and Tested Yield Moments
Beam Specimens - Group W
(Based on dynamic tensile stresses and a transformed tension flange, calculated by using alternative procedure)

Spec.	w/t (25AK) (1)	F_y (ksi) (2)	$(P_y)_{test}$ (kips) (3)	$(M_y)_{comp}$ (in.-kips) (4)	$(M_y)_{test}$ (in.-kips) (5)	(5)/(4) (6)
3A1AW	9.23	24.57	1.082	3.73	4.19	1.123
3A1BW	9.26	24.57	1.117	3.73	4.33	1.161
3A2AW	9.35	26.18	1.130	3.98	4.38	1.101
3A2BW	9.63	26.18	1.135	3.92	4.40	1.122
3A3AW	9.30	27.80	1.241	4.30	4.81	1.118
3A3BW	9.51	27.80	1.264	4.27	4.90	1.146
3B1AW	28.56	24.57	1.507	11.09	10.99	0.991
3B1BW	28.70	24.57	1.531	11.12	10.72	0.964
3B2AW	28.72	26.18	1.650	11.92	11.55	0.969
3B2BW	28.83	26.18	1.583	11.92	11.08	0.930
3B3AW	28.60	27.80	1.766	12.69	12.36	0.974
3B3BW	28.62	27.80	1.785	12.68	12.49	0.985
3C1AW	63.28	24.57	2.432	22.86	20.67	0.904
3C1BW	63.29	24.57	2.450	22.91	20.83	0.909
3C2AW	63.25	26.18	2.677	24.19	22.75	0.941
3C2BW	63.21	26.18	2.648	24.03	22.51	0.937
3C3AW	63.30	27.80	2.789	25.25	23.71	0.939
3C3BW	36.33	27.80	2.731	25.23	23.21	0.920
Mean						1.007
Standard Deviation						0.092

Note: The simulated stress-strain relationships of 25AK sheet steel as shown in Fig. 3.9 were used for calculating the yield moments ($(M_y)_{comp}$).

Table 3.6

Comparison of Computed and Tested Yield Moments
Beam Specimens - Group Z
(Based on dynamic tensile stresses and a transformed compression flange, calculated by using alternative procedure)

Spec.	w/t (25AK) (1)	F_y (ksi) (2)	$(P_y)_{test}$ (kips) (3)	$(M_y)_{comp}$ (in.-kips) (4)	$(M_y)_{test}$ (in.-kips) (5)	(5)/(4) (6)
3A1AZ	25.62	54.92	1.070	3.75	4.14	1.104
3A1BZ	25.61	54.92	1.111	3.74	4.31	1.152
3A2AZ	25.73	55.88	1.180	3.98	4.57	1.147
3A2BZ	25.66	55.88	1.164	3.98	4.51	1.132
3A3AZ	25.65	56.84	1.238	4.25	4.80	1.128
3A3BZ	25.74	56.84	1.278	4.28	4.95	1.156
3B1AZ	45.95	54.92	1.492	11.20	10.44	0.932
3B1BZ	45.89	54.92	1.550	11.13	10.85	0.975
3B2AZ	45.73	55.88	1.605	11.87	11.24	0.947
3B2BZ	45.82	55.88	1.611	11.90	11.27	0.947
3B3AZ	45.73	56.84	1.728	12.71	12.10	0.952
3B3BZ	45.78	56.84	1.680	12.73	11.76	0.924
3C1AZ	82.32	54.92	2.800	26.89	23.80	0.885
3C1BZ	82.38	54.92	2.870	27.13	24.40	0.899
3C2AZ	82.49	55.88	3.012	28.52	25.60	0.898
3C2BZ	82.11	55.88	3.060	28.38	26.01	0.916
3C3AZ	82.41	56.84	3.158	30.14	26.84	0.891
3C3BZ	82.35	56.84	3.140	30.15	26.69	0.885
Mean						0.993
Standard Deviation						0.108

Note: The simulated stress-strain relationships of 25AK sheet steel as shown in Fig. 3.9 were used for calculating the yield moments ($(M_y)_{comp}$).

Table 3.7

Comparison of Computed and Tested Yield Moments
Beam Specimens - Group S
(Based on dynamic tensile stresses and a transformed tension flange, calculated by using alternative procedure)

Spec.	w/t (25AK) (1)	F_y (ksi) (2)	$(P_{y)test}$ (kips) (3)	$(M_y)_{comp}$ (in.-kips) (4)	$(M_y)_{test}$ (in.-kips) (5)	(5)/(4) (6)
3A1AS	24.83	54.92	1.590	10.11	9.14	0.904
3A1BS	24.89	54.92	1.613	10.09	9.27	0.919
3A2AS	24.91	55.88	1.650	10.35	9.49	0.917
3A2BS	24.83	55.88	1.645	10.28	9.46	0.920
3A3AS	24.97	56.84	1.686	10.51	9.69	0.922
3A3BS	24.78	56.84	1.739	10.41	10.00	0.960
3B1AS	42.30	54.92	2.617	20.85	19.95	0.957
3B1BS	42.53	54.92	2.610	20.55	19.90	0.969
3B2AS	42.45	55.88	2.752	20.83	20.98	1.007
3B2BS	42.24	55.88	2.741	20.95	20.90	0.998
3B3AS	42.47	56.84	2.798	21.15	21.33	1.008
3B3BS	42.49	56.84	2.875	21.16	21.92	1.036
3C1AS	69.55	54.92	3.425	32.02	29.11	0.909
3C1BS	69.60	54.92	3.371	31.81	28.65	0.901
3C2AS	69.57	55.88	3.620	32.55	30.77	0.945
3C2BS	69.70	55.88	3.582	32.51	30.45	0.937
3C3AS	69.29	56.84	3.653	32.24	31.05	0.963
3C3BS	69.52	56.84	3.599	32.77	30.59	0.933
Mean						0.950
Standard Deviation						0.040

Note: The simulated stress-strain relationships of 50SK sheet steel as shown in Fig. 3.9 were used for calculating the yield moments ($(M_y)_{comp}$).

Table 3.8

Comparison of Computed and Tested Yield Moments
Beam Specimens - Group K
(Based on dynamic tensile stresses and a transformed compression flange, calculated by using alternative procedure)

Spec.	w/t (25AK) (1)	F_y (ksi) (2)	(P_y)test (kips) (3)	$(M_y)_{comp}$ (in.-kips) (4)	$(M_y)_{test}$ (in.-kips) (5)	(5)/(4) (6)
3A1AK	37.22	24.57	1.540	10.01	8.86	0.885
3A1BK	37.21	24.57	1.532	10.10	8.81	0.872
3A2AK	37.28	26.18	1.590	10.26	9.14	0.891
3A2BK	37.09	26.18	1.610	10.31	9.26	0.898
3A3AK	37.30	27.80	1.692	10.51	9.73	0.926
3A3BK	37.21	27.80	1.670	10.45	9.60	0.919
3B1AK	53.47	24.57	2.630	23.71	20.05	0.846
3B1BK	53.81	24.57	2.615	23.78	19.94	0.839
3B2AK	53.74	26.18	2.700	23.78	20.59	0.866
3B2BK	53.74	26.18	2.714	23.92	20.69	0.865
3B3AK	53.76	27.80	2.758	24.31	21.03	0.865
3B3BK	53.82	27.80	2.816	24.34	21.47	0.882
3C1AK	79.42	24.57	3.987	39.57	33.90	0.857
3C1BK	79.40	24.57	4.052	39.68	34.44	0.868
3C2AK	79.28	26.18	4.172	40.71	35.46	0.871
3C2BK	79.46	26.18	4.203	40.49	35.73	0.882
3C3AK	79.45	27.80	4.298	41.15	36.53	0.888
3C3BK	79.46	27.80	4.301	41.22	36.56	0.887
Mean						0.878
Standard Deviation						0.022

Note: The simulated stress-strain relationships of 50SK sheet steel as shown in Fig. 3.9 were used for calculating the yield moments ($(M_y)_{comp}$).

Table 3.9

Comparison of Computed and Tested Yield Moments
Beam Specimens - Group S
(Based on dynamic compressive stresses and a transformed tension flange, calculated by using Equation 3.5)

Spec.	w/t (25AK) (1)	F_y (ksi) (2)	$(P_{y)test}$ (kips) (3)	$(M_y)_{comp}$ (in.-kips) (4)	$(M_y)_{test}$ (in.-kips) (5)	(5)/(4) (6)
3A1AS	24.83	53.30	1.590	9.44	9.14	0.968
3A1BS	24.89	53.30	1.613	9.43	9.27	0.983
3A2AS	24.91	54.61	1.650	9.75	9.49	0.974
3A2BS	24.83	54.61	1.645	9.68	9.46	0.977
3A3AS	24.97	55.92	1.686	9.97	9.69	0.972
3A3BS	24.78	55.92	1.739	9.87	10.00	1.012
3B1AS	42.30	53.30	2.617	19.81	19.95	1.007
3B1BS	42.53	53.30	2.610	19.52	19.90	1.019
3B2AS	42.45	54.61	2.752	19.90	20.98	1.054
3B2BS	42.24	54.61	2.741	20.01	20.90	1.044
3B3AS	42.47	55.92	2.798	20.33	21.33	1.049
3B3BS	42.49	55.92	2.875	20.35	21.92	1.077
3C1AS	69.55	53.30	3.425	30.73	29.11	0.947
3C1BS	69.60	53.30	3.371	30.53	28.65	0.938
3C2AS	69.57	54.61	3.620	31.40	30.77	0.980
3C2BS	69.70	54.61	3.582	31.36	30.45	0.971
3C3AS	69.29	55.92	3.653	31.28	31.05	0.993
3C3BS	69.52	55.92	3.599	31.79	30.59	0.962
Mean						0.996
Standard Deviation						0.039

Note: Equation 3.5 was used for calculating the yield moments ($(M_y)_{comp}$).

Table 3.10

Comparison of Computed and Tested Yield Moments

Beam Specimens - Group K

(Based on dynamic compressive stresses and a transformed compression flange, calculated by using Equation 3.5)

Spec.	w/t (25AK) (1)	F_y (ksi) (2)	(P_y)test (kips) (3)	$(M_y)_{comp}$ (in.-kips) (4)	$(M_y)_{test}$ (in.-kips) (5)	(5)/(4) (6)
3A1AK	37.22	21.63	1.540	9.35	8.86	0.947
3A1BK	37.21	21.63	1.532	9.44	8.81	0.933
3A2AK	37.28	23.17	1.590	9.66	9.14	0.947
3A2BK	37.09	23.17	1.610	9.71	9.26	0.954
3A3AK	37.30	24.71	1.692	9.97	9.73	0.976
3A3BK	37.21	24.71	1.670	9.91	9.60	0.969
3B1AK	53.47	21.63	2.630	22.58	20.05	0.888
3B1BK	53.81	21.63	2.615	22.64	19.94	0.881
3B2AK	53.74	23.17	2.700	22.88	20.59	0.900
3B2BK	53.74	23.17	2.714	23.01	20.69	0.899
3B3AK	53.76	24.71	2.758	23.46	21.03	0.896
3B3BK	53.82	24.71	2.816	23.49	21.47	0.914
3C1AK	79.42	21.63	3.987	37.30	33.90	0.909
3C1BK	79.40	21.63	4.052	37.39	34.44	0.921
3C2AK	79.28	23.17	4.172	38.06	35.46	0.932
3C2BK	79.46	13.17	4.203	37.83	35.73	0.944
3C3AK	79.45	24.71	4.298	38.02	36.53	0.961
3C3BK	79.46	24.71	4.301	38.08	36.56	0.960
Mean						0.930
Standard Deviation						0.030

Note: Equation 3.5 was used for calculating the yield moments ($(M_y)_{comp}$).

Table 3.11

Comparison of Computed and Tested Yield Moments
Beam Specimens - Group S
(Based on dynamic tensile stresses and a transformed tension flange, calculated by using Equation 3.5)

Spec.	w/t (25AK) (1)	F_y (ksi) (2)	$(P_{y)test}$ (kips) (3)	$(M_y)_{comp}$ (in.-kips) (4)	$(M_y)_{test}$ (in.-kips) (5)	(5)/(4) (6)
3A1AS	24.83	54.92	1.590	9.73	9.14	0.939
3A1BS	24.89	54.92	1.613	9.71	9.27	0.954
3A2AS	24.91	55.88	1.650	9.96	9.49	0.953
3A2BS	24.83	55.88	1.645	9.89	9.46	0.956
3A3AS	24.97	56.84	1.686	10.13	9.69	0.956
3A3BS	24.78	56.84	1.739	10.04	10.00	0.996
3B1AS	42.30	54.92	2.617	20.27	19.95	0.984
3B1BS	42.53	54.92	2.610	19.97	19.90	0.996
3B2AS	42.45	55.88	2.752	20.23	20.98	1.037
3B2BS	42.24	55.88	2.741	20.34	20.90	1.027
3B3AS	42.47	56.84	2.798	20.59	21.33	1.036
3B3BS	42.49	56.84	2.875	20.60	21.92	1.064
3C1AS	69.55	54.92	3.425	31.41	29.11	0.927
3C1BS	69.60	54.92	3.371	31.21	28.65	0.918
3C2AS	69.57	55.88	3.620	31.90	30.77	0.965
3C2BS	69.70	55.88	3.582	31.85	30.45	0.956
3C3AS	69.29	56.84	3.653	31.65	31.05	0.981
3C3BS	69.52	56.84	3.599	32.17	30.59	0.951
Mean						0.978
Standard Deviation						0.041

Note: Equation 3.5 was used for calculating the yield moments ($(M_y)_{comp}$).

Table 3.12

Comparison of Computed and Tested Yield Moments
Beam Specimens - Group K
(Based on dynamic tensile stresses and a transformed compression flange, calculated by using Equation 3.5)

Spec.	w/t (25AK) (1)	F_y (ksi) (2)	(P_y)test (kips) (3)	$(M_y)_{comp}$ (in.-kips) (4)	$(M_y)_{test}$ (in.-kips) (5)	(5)/(4) (6)
3A1AK	37.22	24.57	1.540	9.64	8.86	0.920
3A1BK	37.21	24.57	1.532	9.73	8.81	0.906
3A2AK	37.28	26.18	1.590	9.88	9.14	0.925
3A2BK	37.09	26.18	1.610	9.93	9.26	0.932
3A3AK	37.30	27.80	1.692	10.13	9.73	0.961
3A3BK	37.21	27.80	1.670	10.07	9.60	0.953
3B1AK	53.47	24.57	2.630	23.20	20.05	0.864
3B1BK	53.81	24.57	2.615	23.26	19.94	0.857
3B2AK	53.74	26.18	2.700	23.35	20.59	0.882
3B2BK	53.74	26.18	2.714	23.48	20.69	0.881
3B3AK	53.76	27.80	2.758	23.78	21.03	0.884
3B3BK	53.82	27.80	2.816	23.81	21.47	0.912
3C1AK	79.42	24.57	3.987	37.60	33.90	0.902
3C1BK	79.40	24.57	4.052	37.69	34.44	0.914
3C2AK	79.28	26.18	4.172	38.14	35.46	0.930
3C2BK	79.46	26.18	4.203	37.91	35.73	0.942
3C3AK	79.45	27.80	4.298	37.87	36.53	0.965
3C3BK	79.46	27.80	4.301	37.93	36.56	0.964
Mean						0.916
Standard Deviation						0.034

Note: Equation 3.5 was used for calculating the yield moments ($(M_y)_{comp}$).

Table 3.13

Comparison of Computed and Tested Yield Moments
Beam Specimens - Group W
(Based on dynamic tensile stresses and a transformed tension flange, calculated by using Equation 3.5)

Spec.	w/t (25AK) (1)	F_y (ksi) (2)	$(P_y)_{test}$ (kips) (3)	$(M_y)_{comp}$ (in.-kips) (4)	$(M_y)_{test}$ (in.-kips) (5)	(5)/(4) (6)
3A1AW	9.23	21.63	1.082	3.03	4.19	1.382
3A1BW	9.26	21.63	1.117	3.03	4.33	1.429
3A2AW	9.35	23.17	1.130	3.23	4.38	1.356
3A2BW	9.63	23.17	1.135	3.19	4.40	1.377
3A3AW	9.30	24.71	1.241	3.45	4.81	1.395
3A3BW	9.51	24.71	1.264	3.44	4.90	1.429
3B1AW	28.56	21.63	1.507	9.47	10.99	1.160
3B1BW	28.70	21.63	1.531	9.50	10.72	1.128
3B2AW	28.72	23.17	1.650	10.16	11.55	1.137
3B2BW	28.83	23.17	1.583	10.16	11.08	1.090
3B3AW	28.60	24.71	1.766	10.70	12.36	1.155
3B3BW	28.62	24.71	1.785	10.70	12.49	1.167
3C1AW	63.28	21.63	2.432	20.12	20.67	1.027
3C1BW	63.29	21.63	2.450	20.16	20.83	1.033
3C2AW	63.25	23.17	2.677	21.19	22.75	1.074
3C2BW	63.21	23.17	2.648	21.07	22.51	1.068
3C3AW	63.30	24.71	2.789	21.95	23.71	1.080
3C3BW	36.33	24.71	2.731	21.94	23.21	1.058
Mean						1.197
Standard Deviation						0.150

Note: Equation 3.5 was used for calculating the yield moments ($(M_y)_{comp}$).

Table 3.14

Comparison of Computed and Tested Yield Moments
Beam Specimens - Group Z
(Based on dynamic tensile stresses and a transformed
coompression flange, calculated by using Equation 3.5)

Spec.	w/t (25AK) (1)	F_y (ksi) (2)	$(P_y)_{test}$ (kips) (3)	$(M_y)_{comp}$ (in.-kips) (4)	$(M_y)_{test}$ (in.-kips) (5)	(5)/(4) (6)
3A1AZ	25.62	54.92	1.070	3.04	4.14	1.360
3A1BZ	25.61	54.92	1.111	3.04	4.31	1.418
3A2AZ	25.73	55.88	1.180	3.24	4.57	1.412
3A2BZ	25.66	55.88	1.164	3.23	4.51	1.394
3A3AZ	25.65	56.84	1.238	3.42	4.80	1.403
3A3BZ	25.74	56.84	1.278	3.44	4.95	1.440
3B1AZ	45.95	54.92	1.492	9.55	10.44	1.093
3B1BZ	45.89	54.92	1.550	9.50	10.85	1.142
3B2AZ	45.73	55.88	1.605	10.11	11.24	1.111
3B2BZ	45.82	55.88	1.611	10.13	11.27	1.113
3B3AZ	45.73	56.84	1.728	10.72	12.10	1.128
3B3BZ	45.78	56.84	1.680	10.73	11.76	1.095
3C1AZ	82.32	54.92	2.800	23.61	23.80	1.008
3C1BZ	82.38	54.92	2.870	23.78	24.40	1.026
3C2AZ	82.49	55.88	3.012	25.29	25.60	1.012
3C2BZ	82.11	55.88	3.060	25.18	26.01	1.033
3C3AZ	82.41	56.84	3.158	26.69	26.84	1.006
3C3BZ	82.35	56.84	3.140	26.70	26.69	1.000
Mean						1.177
Standard Deviation						0.171

Note: Equation 3.5 was used for calculating the yield moments ($(M_y)_{comp}$).

Table 3.15

Ratios of Tested to Computed Yield Moments

group	based on dynamic yield stresses	M_y is computed by applying the calculation procedure discussed in the 20th P. R. (using real stress-strain curves). Refer Tables 4.4 through Table 4.12 of 20th P. R..		M_y is computed by applying the calculation procedure discussed in this report (using transformed sections and simulated stress-strain curves).		M_y is computed by applying AISI Formulas - Equation 3.5 (using transformed sections). Refere Tables 3.9 through Table 3.12 of this report.	
		mean value	standard deviation	mean value	standard deviation	mean value	standard deviation
W	tensile	0.993	0.088	1.007	0.092		
W	comp.	1.113	0.110	1.140	0.119		
Z	tensile	0.988	0.096	0.993	0.108		
Z	comp.	1.116	0.110	1.133	0.127		
S	tensile	0.942	0.040	0.950	0.040	0.978	0.041
S	comp.	0.974	0.040	0.972	0.038	0.996	0.039
K	tensile	0.884	0.014	0.878	0.022	0.916	0.034
K	comp.	0.920	0.019	0.894	0.025	0.930	0.030

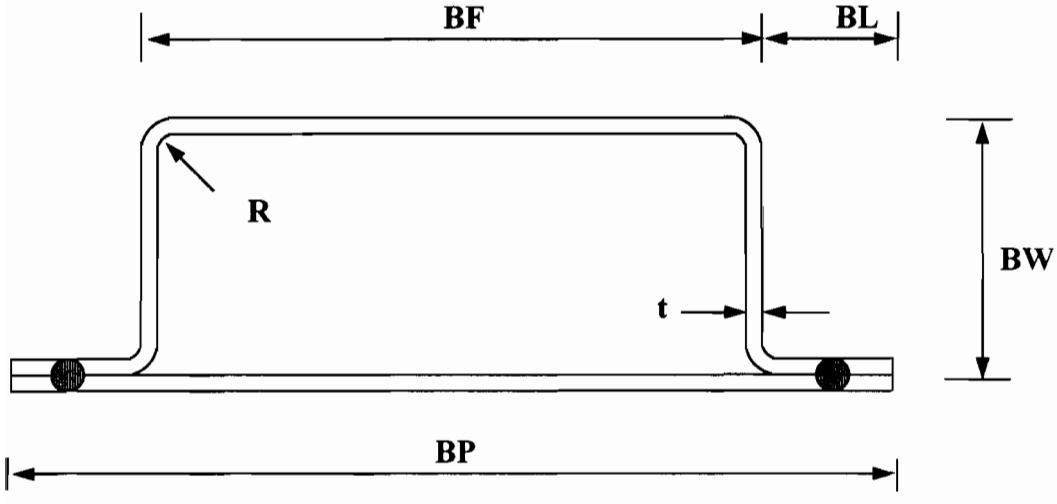

Figure 2.1 Configuration of Hybrid Beam Specimen

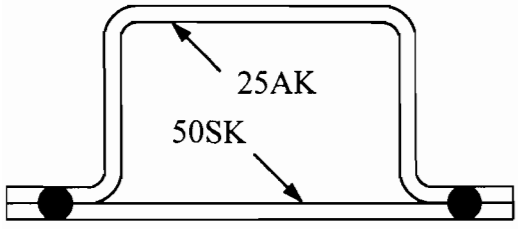

Group W

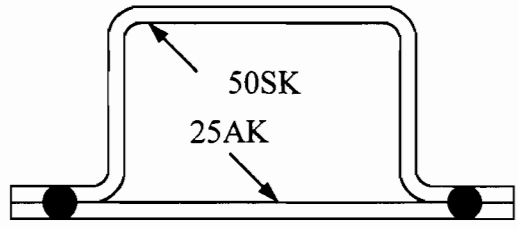

Group S

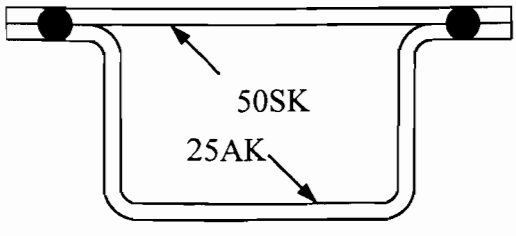

Group Z

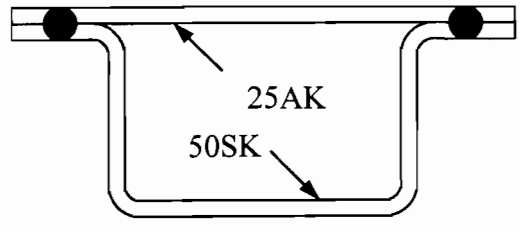

Group K

Figure 2.2 Cross Section of Hybrid Beams Used in This Study

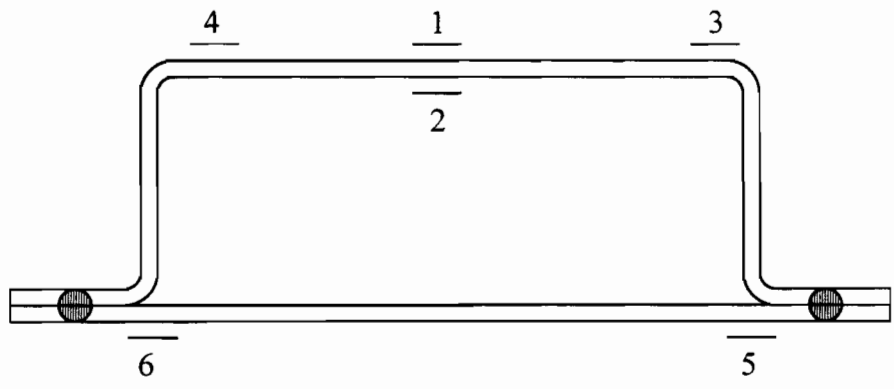

(a) Group W and Group S

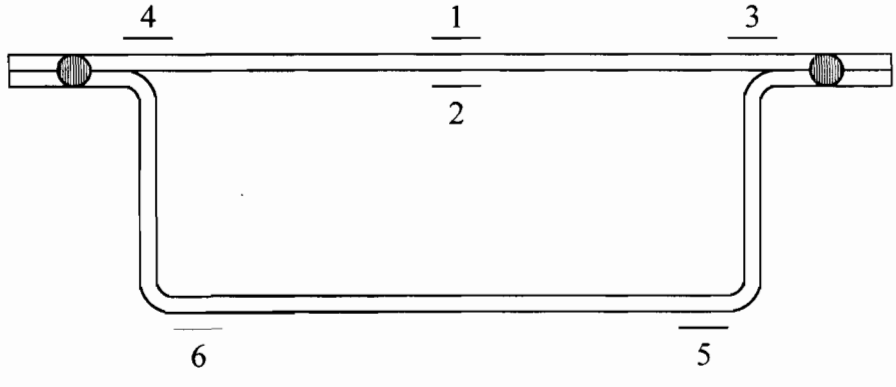

(b) Group Z and Group K

Figure 2.3 Locations of Strain Gages at Midspan Section of Beams

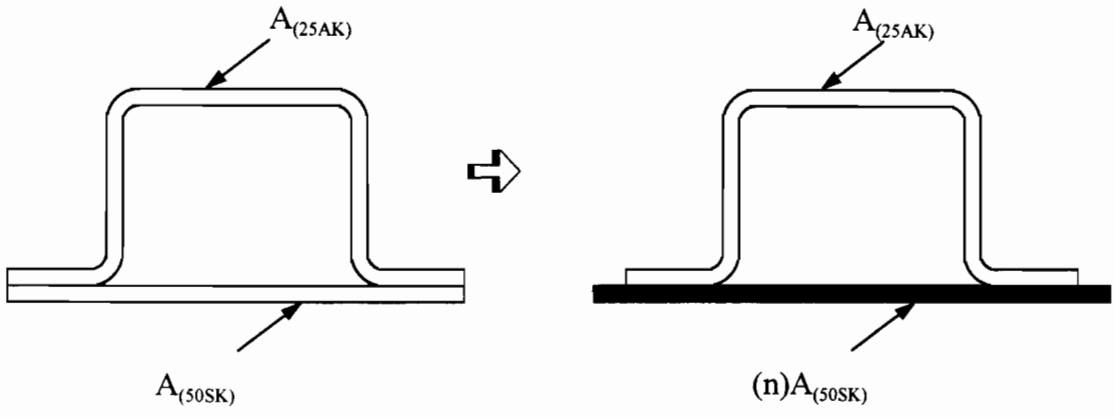

Group W

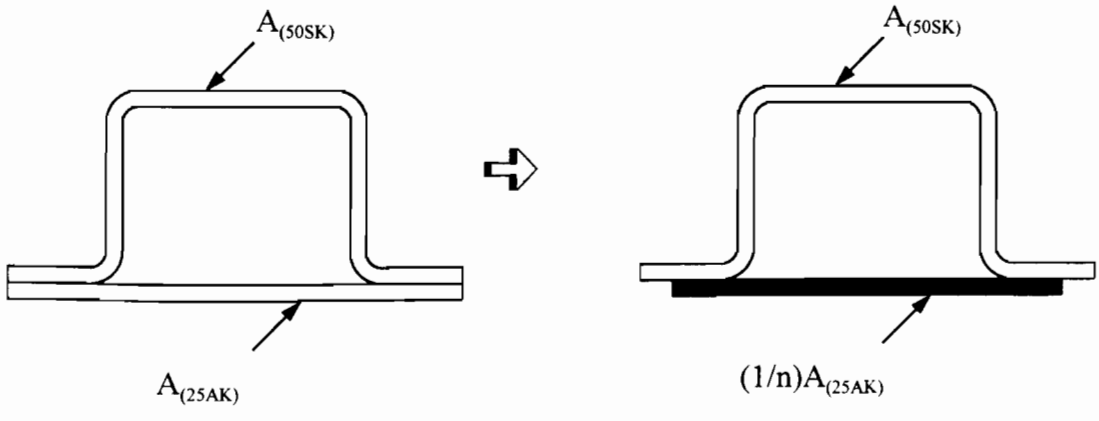

Group S

Figure 3.1a Cross Section of Transformed Section

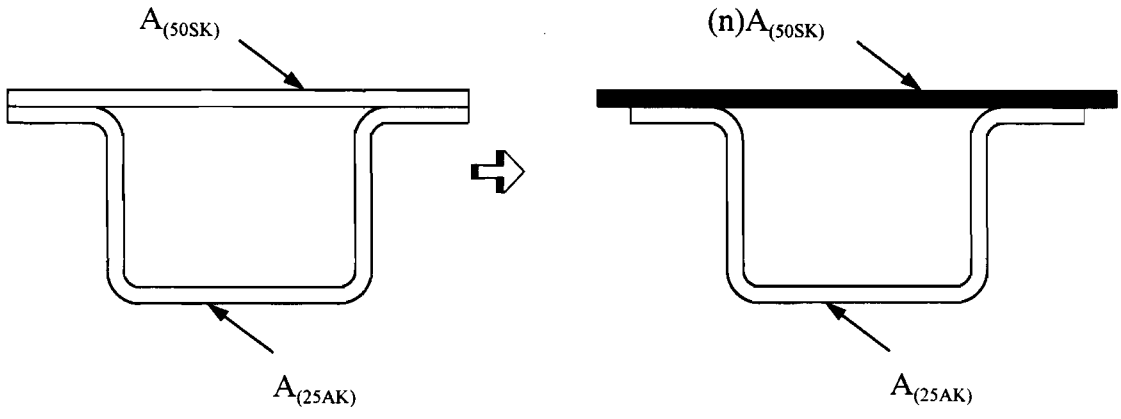

Group Z

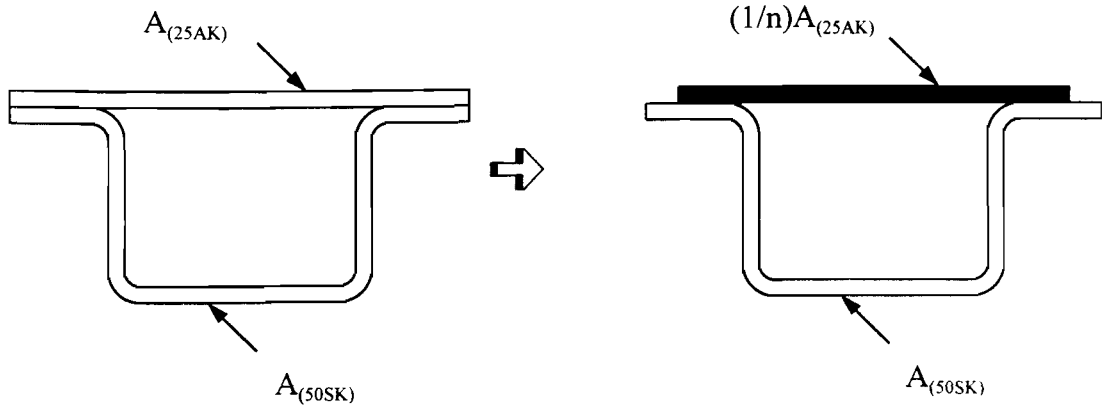

Group K

Figure 3.1b Cross Section of Transformed Section

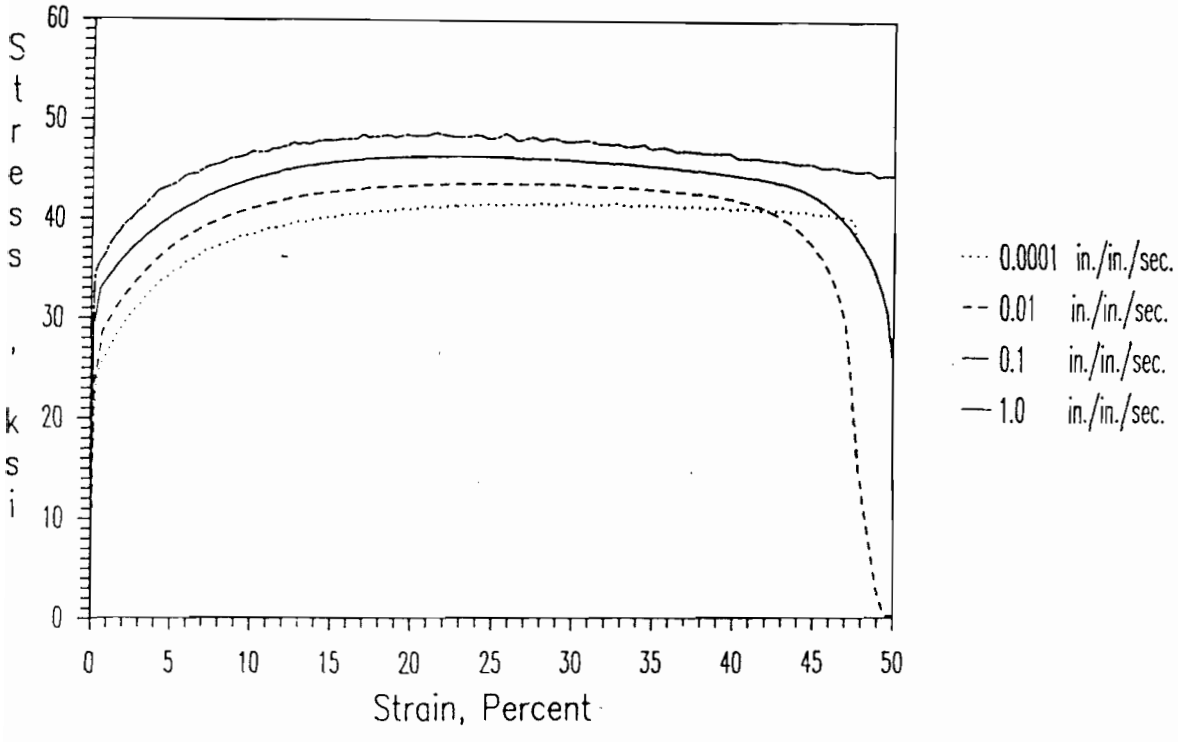

Figure 3.2 Stress-Strain Curves for 25 AK Sheet Steel in Longitudinal Tension under Different Strain Rates

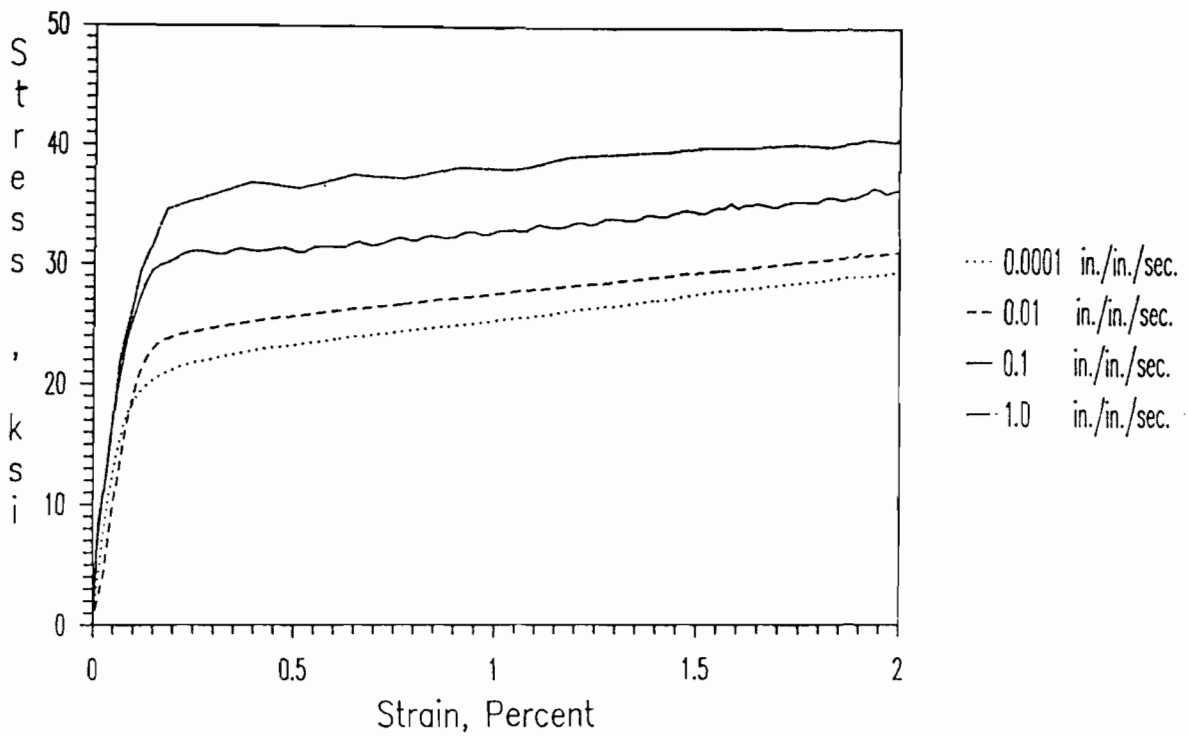

Figure 3.3 Stress-Strain Curves for 25 AK Sheet Steel in Longitudinal Compression under Different Strain Rates

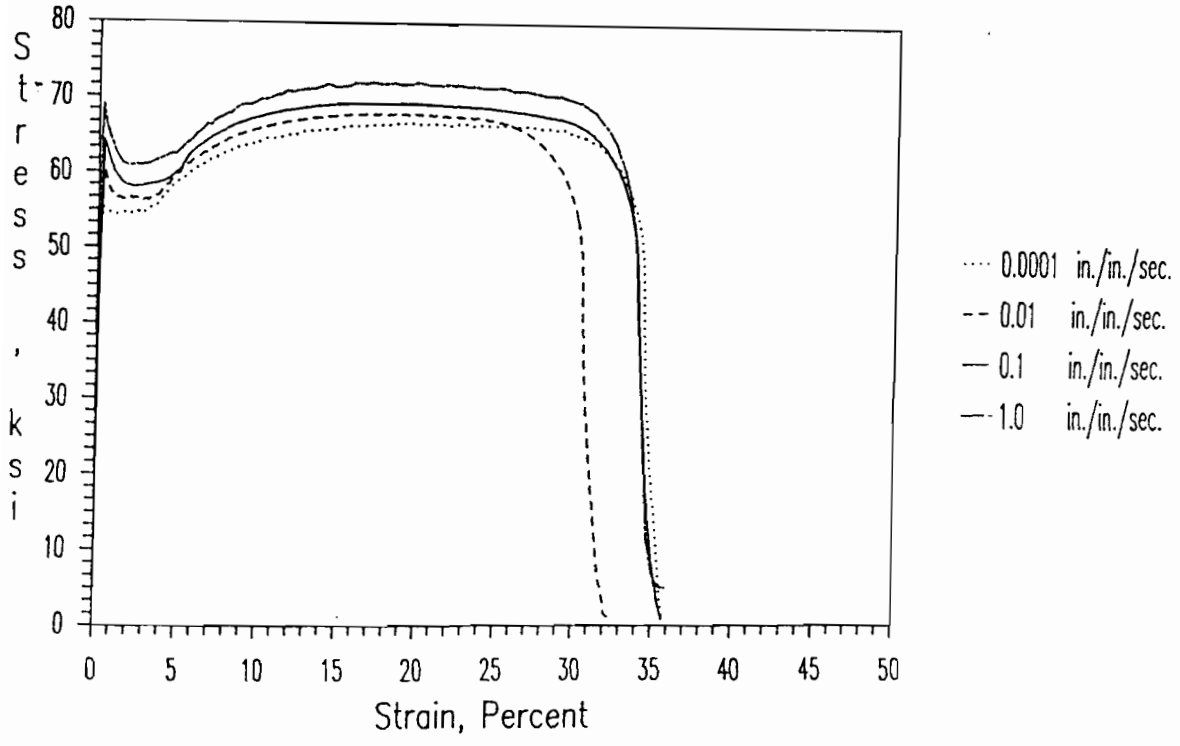

Figure 3.4 Stress-Strain Curves for 50 SK Sheet Steel in Longitudinal Tension under Different Strain Rates

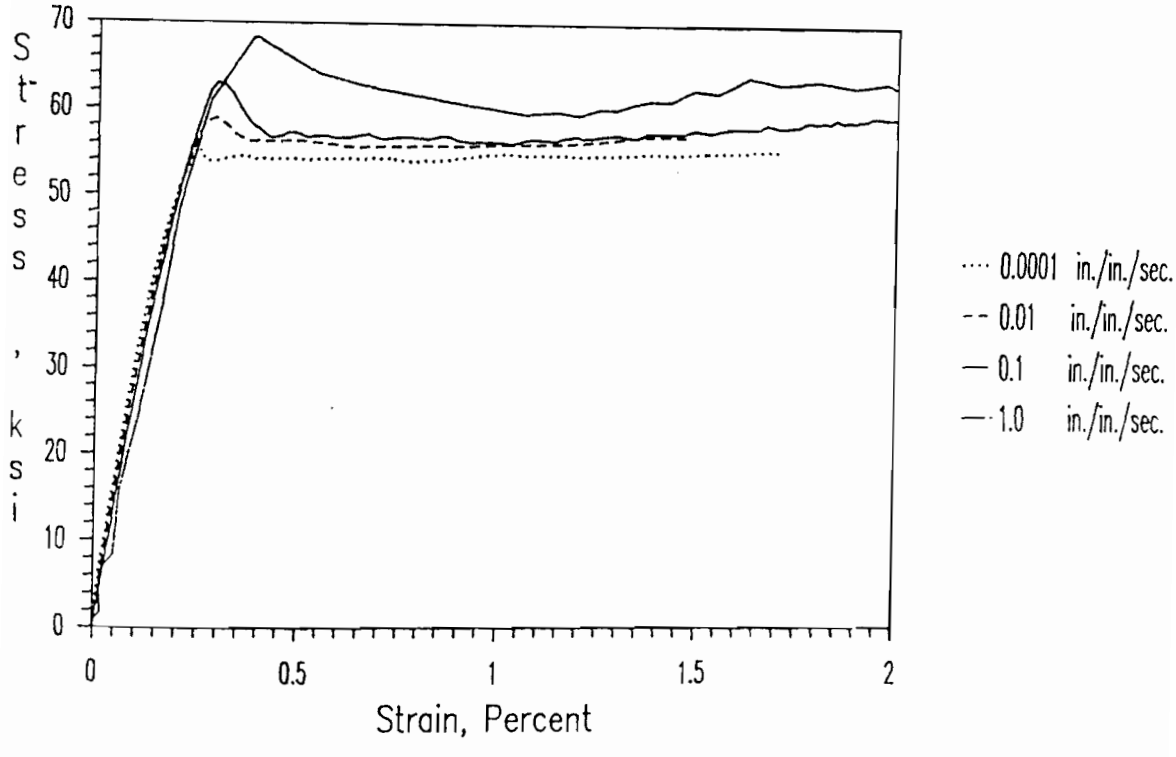

Figure 3.5 Stress-Strain Curves for 50SK Sheet Steel in Longitudinal Compression under Different Strain Rates

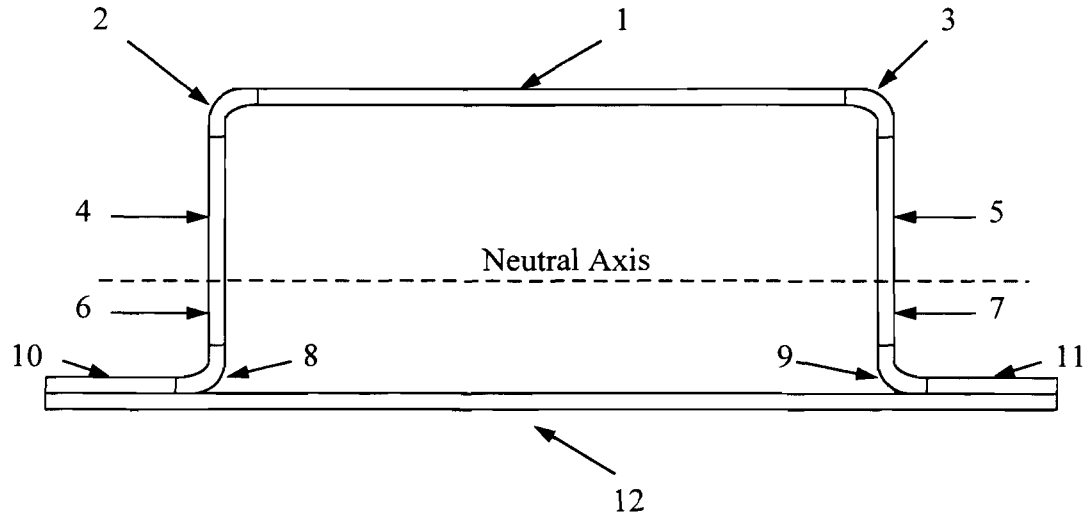

Figure 3.6 Location of Elements for Determination of the Neutral Axis of a Beam Specimen

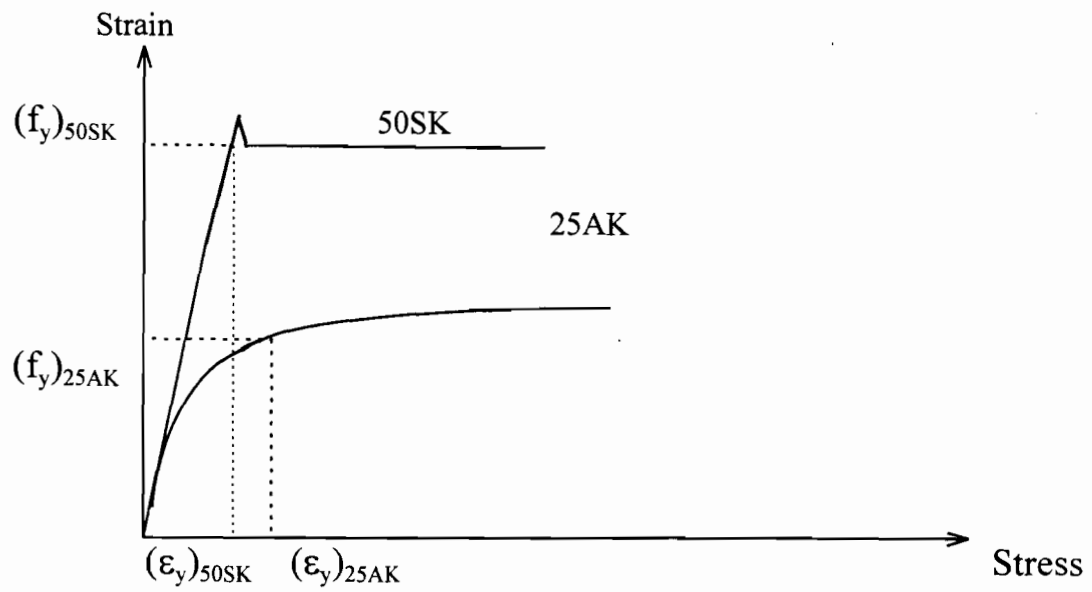

Figure 3.7 Schematic Sketch of Stress-Strain Relationships for 25AK and 50SK Sheet Steels

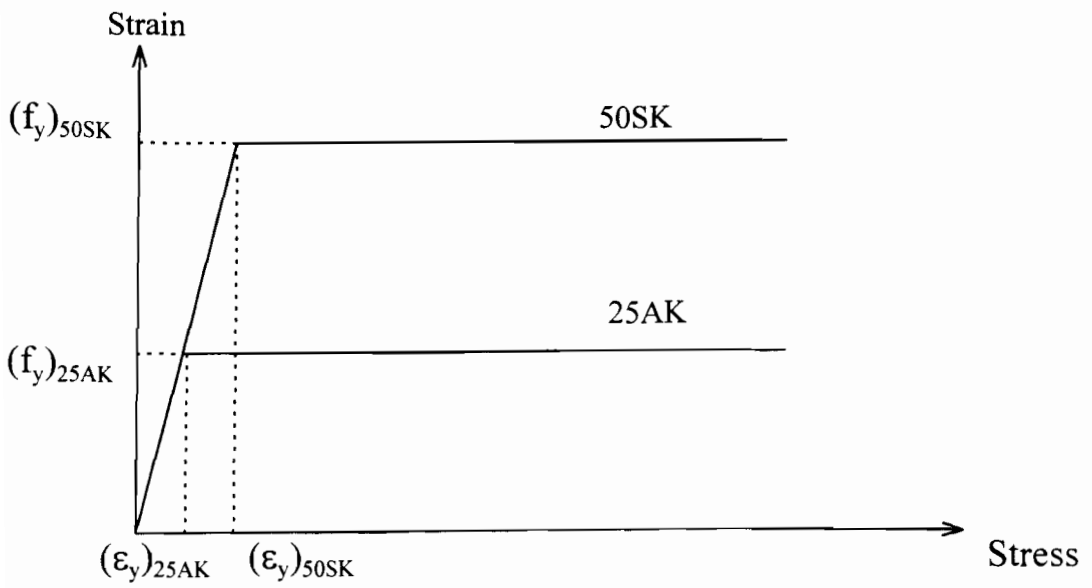

Figure 3.8 Approximate Stress-Strain Relationships for 25AK and 50SK Sheet Steels

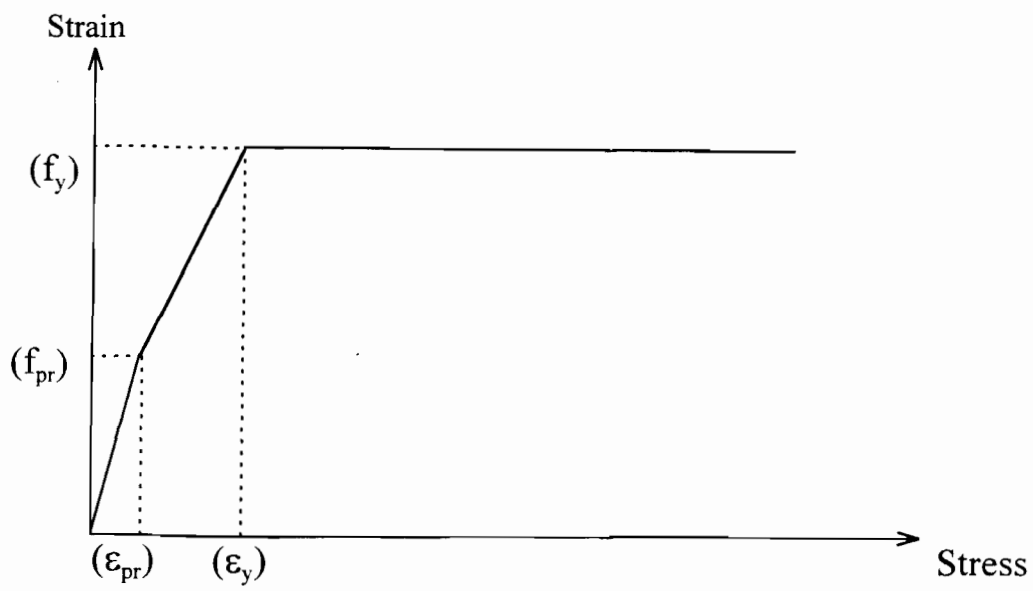

Figure 3.9 Simulated Stress-Strain Relationships for 25AK and 50SK Sheet Steels

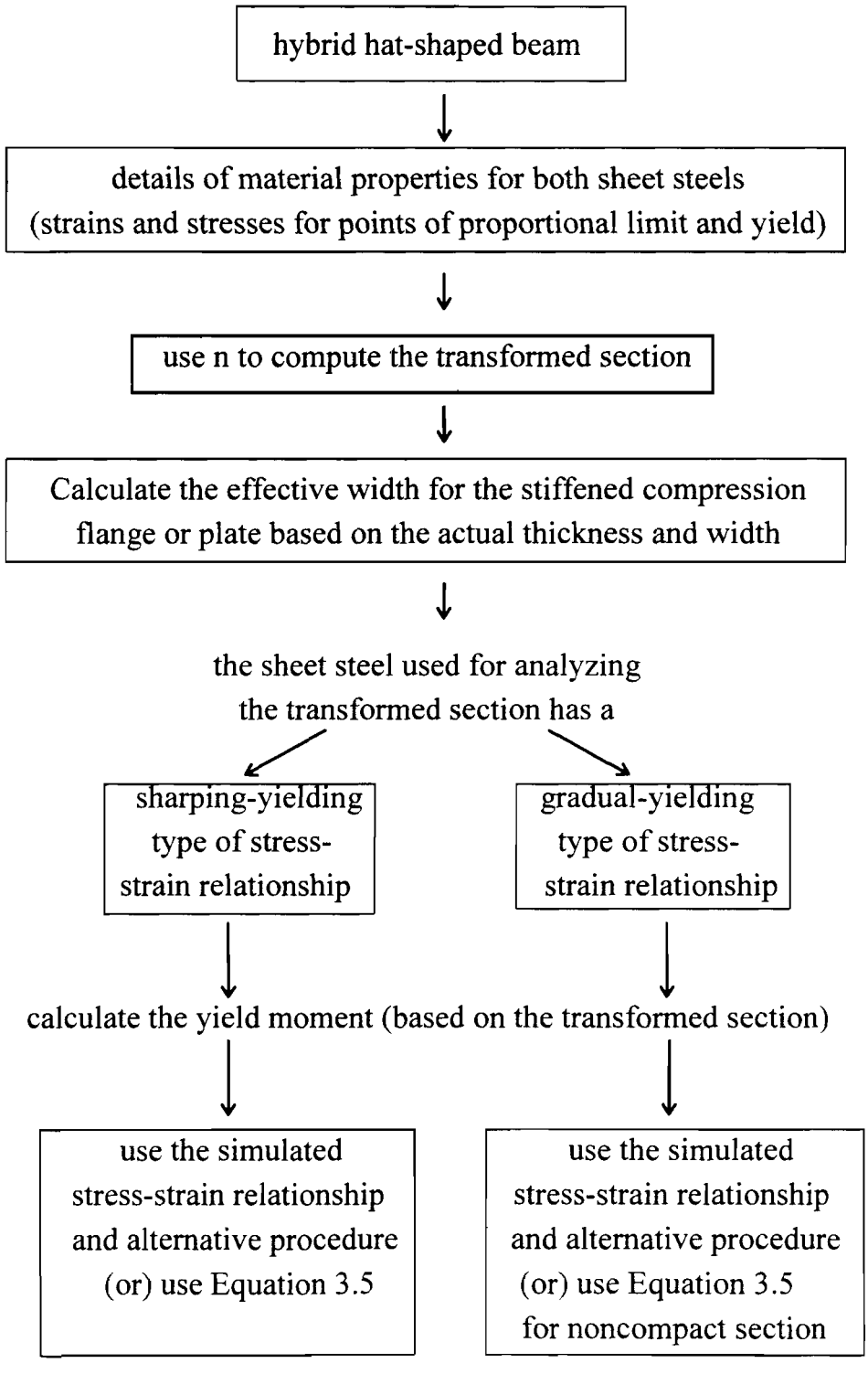

Figure 3.10 Design Procedure for Calculating the Yield Moment of Hybrid Hat-Shaped Beam

NOTATION

The following symbols are used in this report:

b	Effective width of a compression element
E	Modulus of elasticity of steel, 29,500 ksi
f	Edge stress in the compression element
F_{pr}	Proportional limit
F_y	Yield stress
k	Buckling coefficient
L	Span length of beam specimen
$(M_y)_{comp}$	Computed yield moment
$(M_y)_{test}$	Tested yield moment
n	Ratio of the moduli of elasticity
P_y	Yield load
R	Inside bend radius
S_e	Elastic section modulus of effective section
t	Thickness of element
w	Flat width of a compression element
λ	Slenderness factor
μ	Poisson's ratio
ε_{pr}	Strain under proportional limit
ε_y	Yield Strain
σ_{pr}	Proportional limit

σ_y Yield point